Inorganic Chemistry

Article

pubs.acs.org/IC

Structural Diversity due to Amino Alcohol Ligands Leading to Rare μ_4-Hydroxo-Bridged Tetranuclear and "Bicapped Cubane" Cores in Copper(II) Complexes: A Theoretical and Experimental Magnetostructural Study

Petri Seppälä,[†] Enrique Colacio,*[,‡] Antonio J. Mota,[‡] and Reijo Sillanpää*[,†]

[†]Department of Chemistry, University of Jyväskylä, P.O. Box 35, University of Jyväskylä, FIN-40014 Jyväskylä, Finland

[‡]Departamento de Química Inorgánica, Facultad de Ciencias, Universidad de Granada, Avda. de Fuentenueva s/n, 18071 Granada, Spain

Supporting Information

ABSTRACT: The μ_4-hydroxo- and alkoxo-bridged tetranuclear copper(II) complexes, $[Cu_4(\mu_4\text{-}OH)(dmae)_4][Ag(NO_3)_4]$ (**1**), $[Cu_4(\mu_4\text{-}OH)(dmae)_4][Na(NO_3)_4]$ (**2**), $[Cu_4(\mu_4\text{-}OH)(dmae)_4][K(NO_3)_4]$ (**3**), and hexanuclear alkoxo-bridged "bicapped cubane" copper(II) complex $[Cu_6(ae)_8(ClO_4)_2](ClO_4)_2\cdot MeOH$ (**8**) (dmae = *N*,*N*-dimethylaminoethanolato and ae = 2-aminoethanolato) were synthesized via self-assembly from chelating amino alcohols and copper(II), silver (**1**), sodium (**2**), and potassium (**3**) nitrates or copper(II) perchlorate (**8**). The complexes are characterized by elemental analyses, single-crystal X-ray diffraction, and variable temperature magnetic measurements. The crystal structures of complexes **1**−**3** consist of almost planar tetranuclear $[Cu_4(\mu_4\text{-}OH)(dmae)_4]^{3+}$ units, in which Cu(II) ions are also weakly bonded to nitrate anions. The adjacent tetranuclear units of **1**−**3** are connected by ionic interactions between nitrate anions and sodium, potassium, or silver cations resulting in the formation of 1D polymers. The crystal structure of **8** consists of hexanuclear $[Cu_6(ae)_8]^{4+}$ "bicapped cubane" units, in which the capping Cu(II) ions are weakly bonded to perchlorate anions. The adjacent hexanuclear units of **8** are connected by hydrogen bonds resulting in the formation of 3D hydrogen bonded networks. Also the results from the synthetic studies leading to the formation of new copper(II) and silver(I) complexes (**4**−**7**) using Hae, 3-aminopropanol (Hap), and *N*,*N*-dimethylaminopropanol (Hdmap) in similar reactions, which gave tetra- and hexanuclear complexes, are presented. Experimental magnetic studies showed that complexes **1** and **2** exhibit dominant antiferromagnetic coupling leading to an $S = 0$ ground state, whereas **8** exhibits a large dominant antiferromagnetic interaction between the capping copper atoms and the copper atoms of the top and bottom faces of the cubane unit that define two isosceles triangles. This interaction leads to an $S = 1/2$ ground state for each triangle. The weak ferromagnetic interaction between these doublet states through the cubane unit leads to a triplet $S = 1$ ground state for **8**. The values of the magnetic exchange coupling constant were the following: $J = +1.8$ (**1**) and $+2.9$ cm^{-1} (**2**) between adjacent copper atoms; $J' = -29.2$ (**1**) and -32.2 cm^{-1} (**2**) between opposite copper atoms; $J = -297.6$ cm^{-1} and $zJ' = +0.07$ cm^{-1} (**8**). Magnetic coupling constants calculated for **2** and **8** by DFT methods are in general of the same nature and magnitude as the experimental ones.

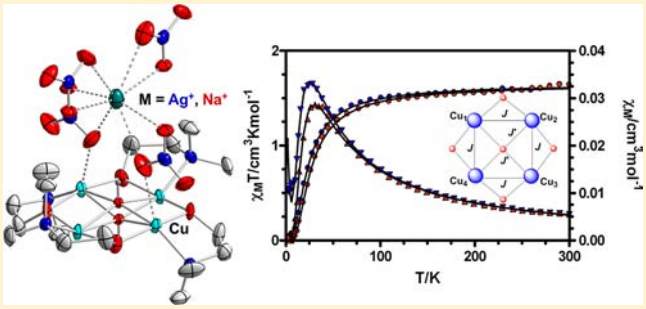

INTRODUCTION

The coordination chemistry of polynuclear copper(II) complexes has received much attention in the past decades due to their interesting architectures and potential applications in the fields of coordination polymers,[1] magnetochemistry,[2] bioinorganic chemistry,[3] and catalysis.[4] The inexpensive and commercially available multidentate amino alcohols have been broadly used for the preparation of polynuclear copper(II) complexes through a self-assembly process, since the hydroxyl groups of amino alcohols can be easily deprotonated in the presence of copper(II) salts and the resulting alkoxo groups act as a bridge leading to the formation of dimeric,[5] dinuclear,[6] trinuclear,[7] tetranuclear,[8] hexanuclear,[9] octanuclear,[10] and nonanuclear[11] copper(II) clusters, coordination polymers, and supramolecular frameworks.

Furthermore, alkoxo-bridged polynuclear copper(II) complexes act as model systems allowing a better understanding of the magnetic interactions between the metal centers, since the single unpaired electron on each copper(II) ion forms a relatively simple magnetic exchange system. The magnetic behavior of hydroxo- and alkoxo-bridged polynuclear copper(II) complexes is well-known from experimental[12] and theoretical studies.[13] Hatfield, Hodgson, and co-workers[12b]

Received: May 27, 2013
Published: September 16, 2013

   dx.doi.org/10.1021/ic401325b | *Inorg. Chem.* 2013, 52, 11096−11109

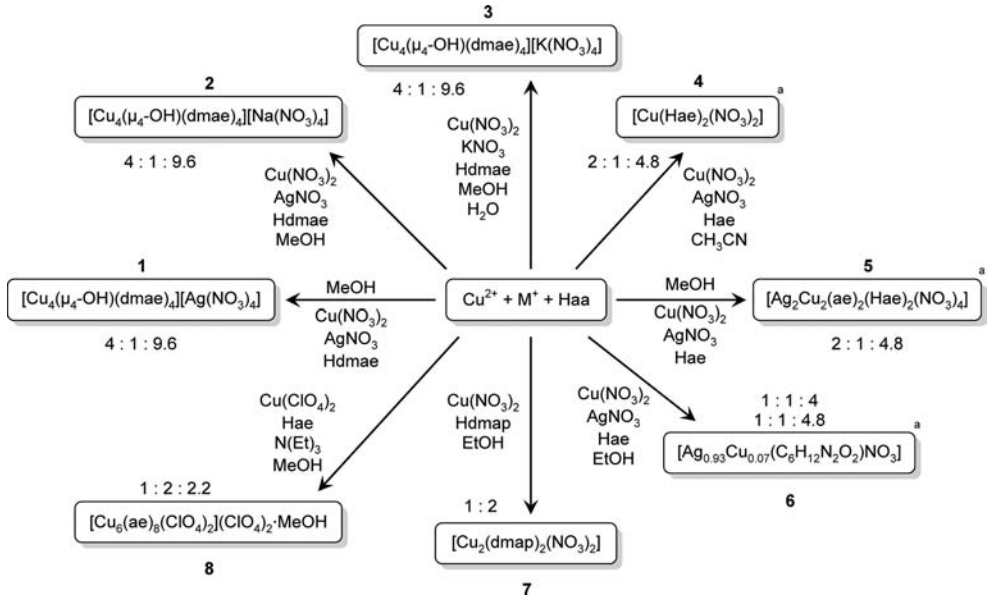

Figure 1. Schematic synthetic routes for **1**–**8**, including the stoichiometric ratios of the starting materials (Cu/M/Hae for **1**–**3**, M = Ag, Na, or K; Cu/M/Hae for **4**–**6**, M = Ag; Cu/Hdmap for **7**; Cu/Hae/N(Et)$_3$ for **8**). Haa = amino alcohol, Hae = aminoethanol, Hdmae = dimethylaminoethanol, and Hdmap = diaminopropanol. [a]Side product; the main product is $[Cu(ae)(Hae)]_2(NO_3)_2$.

established that the primary geometric factor determining the magnitude of the exchange coupling for dinuclear complexes was the Cu–O–Cu bridging angle (θ). The larger the θ angle, the stronger the antiferromagnetic coupling between the copper(II) ions. Theoretical studies of dinuclear, trinuclear, and tetranuclear complexes by Ruiz et al.[13c,h,i] showed that, although the θ angle is the single most important parameter, other geometric factors such as the planarity of the coordination sphere around the copper(II) ions and the out-of-plane shift of the carbon atom of the bridging alkoxo group (H atom for hydroxo complexes) also played a significant role in determining the sign and magnitude of the exchange coupling.

The most common structural types for tetranuclear copper(II) complexes are cubane-like Cu_4O_4 core and $Cu_4(\mu_4\text{-}O)$ tetrahedron,[14] and a few examples of tetranuclear $Cu_4(\mu_4\text{-}OH)$ core have also been reported.[15] The cubane-like Cu_4O_4 core is the most common among tetranuclear alkoxo-bridged copper(II) amino alcohol complexes, whereas only a few structures with a $Cu_4(\mu_4\text{-}O)$ tetrahedron have been reported.[8k,l,o] In these complexes, the central μ_4-oxygen atom is surrounded by four copper atoms forming a distorted tetrahedral environment around the μ_4-oxygen atom. In the hexanuclear heterobimetallic Cu–Cd[8k,o] and Cu–Zn[8o] complexes the metal centers are further connected by bridging amino alcohols and acetates, whereas in the tetranuclear copper complex,[8l] the copper centers are clustered through bridges between amino alcohols and μ_3-B-OH groups (converted from $[BF_4]^-$ in alkalic medium). To the best of our knowledge, structures of planar tetranuclear alkoxo-bridged copper(II) complexes with $Cu_4(\mu_4\text{-}OH)$ cores have not been reported.

Within this framework and to enrich the structural diversity of copper(II) complexes with amino alcohols and as an extension to our previous studies[12k–m] of dinuclear and trinuclear alkoxo-bridged copper(II) complexes, the syntheses, crystal structures, and magnetic properties (experimental for **1** and both experimental and theoretical for **2**) for three new planar tetranuclear μ_4-hydroxo- and alkoxo-bridged $[Cu_4(\mu_4\text{-}OH)(dmae)_4][Ag(NO_3)_4]$ (**1**), $[Cu_4(\mu_4\text{-}OH)(dmae)_4][Na(NO_3)_4]$ (**2**), and $[Cu_4(\mu_4\text{-}OH)(dmae)_4][K(NO_3)_4]$ (**3**) (dmae = *N*,*N*-dimethylaminoethanolato) cores in copper(II) complexes are presented. Complexes **1**–**3** represent rare tetranuclear copper compounds with a $Cu_4(\mu_4\text{-}OH)$ core, the first examples with a small amino alcohol as a ligand. This structure type has been reported only on a few occasions for the complexes with Robson-type macrocyclic[15a,b] and 2-aminoglucose[15c] ligands and in carbonato-copper(II) anion.[15d]

In addition, syntheses similar to those that produced **1**–**3** were also carried out using 2-aminoethanol (Hae), 3-aminopropanol (Hap), and *N*,*N*-dimethylaminopropanol (Hdmap) in order to test whether they would act as similar complex forming agents as Hdmae. The schematic diagram of the productive syntheses is depicted in Figure 1. As the results of these syntheses, two new copper(II) amino alcohol complexes, one heterometallic Cu(II)/Ag(I) amino alcohol complex and one silver(I) oxazino-oxazine complex (**4**–**7**) were obtained, $[Cu(Hae)_2(NO_3)_2]$ (**4**), $[Ag_2Cu_2(ae)_2(Hae)_2(NO_3)_4]$ (**5**), $[Ag_{0.93}Cu_{0.07}(C_6H_{12}N_2O_2)NO_3]$ complex (**6**), and $[Cu_2(dmap)_2(NO_3)_2]$ (**7**), and their crystal structures are reported.

Also, the role of the anion was tested using copper(II) perchlorate instead of copper(II) nitrate and Hae. This system produces a new "bicapped cubane"-like hexanuclear alkoxo-bridged copper(II) complex $[Cu_6(ae)_8(ClO_4)_2](ClO_4)_2MeOH$ (**8**). The synthesis, crystal structure, and magnetic properties (both experimental and theoretical) for **8** are also presented. Complex **8** is the third example of a hexanuclear copper(II) cluster with a "bicapped cubane" core, the first one having been derived from 2-amino-2-methylpropanol[9c] and the second recently from a Schiff base ligand.[16] Finally, the magnetic properties (experimental and theoretical) of complexes **1**, **2**, and **8** are presented and discussed.

EXPERIMENTAL SECTION

Materials. All chemicals and solvents were purchased from commercial sources and were used without further purification.

dx.doi.org/10.1021/ic401325b | *Inorg. Chem.* 2013, 52, 11096–11109

Caution! Although we have experienced no difficulties, perchlorate salts of metal complexes with organic ligands are potentially explosive and should be handled with care even in small quantities.

Syntheses. *Synthesis of $[Cu_4(\mu_4\text{-}OH)(dmae)_4][Ag(NO_3)_4]$ (1).* $Cu(NO_3)_2{\cdot}3H_2O$ (193 mg, 0.80 mmol) dissolved in methanol (4 mL) in a test tube and $AgNO_3$ (34.0 mg, 0.20 mmol) dissolved in methanol (2 mL) were mixed. To the formed solution, Hdmae (193 μL, 1.92 mmol) in methanol (4 mL) was added. The solution was allowed to stand in the dark at room temperature. Slow evaporation of the resulting green solution for a week led to the formation of blue crystals suitable for X-ray crystallography. Crystals were filtered and washed with ethanol and diethyl ether and dried in air. Yield 148 mg (75%). FTIR (KBr, cm^{-1}): 3421(m), 1383(s), 1302(s), 1063(s), 1016(m), 951(m), 900(m), 786(m), 651(w), 522(w), 464(w). Anal. calcd for $C_{16}H_{41}Cu_4N_8Ag_1O_{17}$: C, 19.61; H, 4.22; N, 11.44. Found: C, 19.71; H, 4.18; N, 11.61%.

Synthesis of $[Cu_4(\mu_4\text{-}OH)(dmae)_4][Na(NO_3)_4]$ (2). $Cu(NO_3)_2{\cdot}3H_2O$ (193 mg, 0.80 mmol) dissolved in methanol (4 mL) in a test tube and $NaNO_3$ (17.0 mg, 0.20 mmol) dissolved in methanol (1 mL) were mixed. To the formed solution, Hdmae (193 μL, 1.92 mmol) in methanol (4 mL) was added. The resulting green solution was allowed to stand at room temperature. Slow evaporation of the solvent for a week led to the formation of blue crystals suitable for X-ray crystallography. Crystals were filtered and washed with ethanol and diethyl ether and dried in air. Yield 115 mg (64%). FTIR (KBr, cm^{-1}): 3424(m), 1384(s), 1324(s), 1066(s), 1017(m), 953(m), 900(m), 786(m), 651(w), 523(w), 467(w). Anal. calcd for $C_{16}H_{41}Cu_4N_8Na_1O_{17}$: C, 21.48; H, 4.62; N, 12.52. Found: C, 21.54; H, 4.62; N, 12.71%.

Synthesis of $[Cu_4(\mu_4\text{-}OH)(dmae)_4][K(NO_3)_4]$ (3). $Cu(NO_3)_2{\cdot}3H_2O$ (193 mg, 0.80 mmol) dissolved in methanol (4 mL) in a test tube and KNO_3 (20.3 mg, 0.20 mmol) dissolved in methanol–water (4:1, 2 mL) were mixed. To the formed solution, Hdmae (193 μL, 1.92 mmol) in methanol (4 mL) was added. Slow evaporation of the resulting dark green solution for a week led to the formation of blue crystals suitable for X-ray crystallography but also formation of colorless KNO_3 crystals, which were separated mechanically for analyses. The obtained crystals were filtered and washed with ethanol and diethyl ether and dried in air. Anal. calcd for $C_{16}H_{41}Cu_4N_8K_1O_{17}$: C, 21.10; H, 4.54; N, 12.30. Found: C, 21.18; H, 5.03; N, 11.90%.

Synthesis of 4–6. These compounds were isolated as a minor components described in Scheme 1 and the discussion part.

Scheme 1. Magnetic Exchange Pathways in Complexes 1 and 2

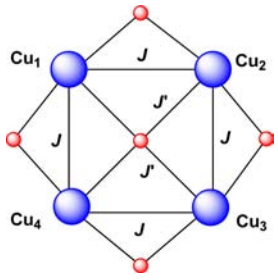

Synthesis of $[Cu_2(dmap)_2(NO_3)_2]$ (7). $Cu(NO_3)_2{\cdot}3H_2O$ (145 mg, 0.60 mmol) was dissolved in ethanol (3 mL), and to this solution, Hdmap (142 μL, 1.2 mmol) in ethanol (3 mL) was added in test tube. A light green precipitate was formed after addition of Hdmap. The resulting light green solution was allowed to stand at room temperature overnight, whereupon well-formed blue crystals suitable for X-ray crystallography were obtained along with a light green precipitate. The light green precipitate and the blue crystals were separated by pipetting the solvent along with the precipitate from the top of the blue crystals. The crystals were filtered and washed with ethanol and diethyl ether and dried in air. Yield 52 mg (19%). Similar yield was obtained if triethylammine was used as a base. Anal. calcd for $C_{10}H_{24}Cu_2N_4O_8$: C, 26.37; H, 5.31; N, 12.30. Found: C, 26.33; H, 5.23; N, 12.31%.

Synthesis of $[Cu_6(ae)_8(ClO_4)_2](ClO_4)_2{\cdot}MeOH$ (8). $Cu(ClO_4)_2{\cdot}6H_2O$ (222 mg, 0.60 mmol) was dissolved in methanol (3 mL) in a test tube. On top of this solution, Hae (72.0 μL, 1.20 mmol) and $N(Et)_3$ (183 μL, 1.32 mmol) in methanol (3 mL) were carefully added to avoid the mixing of the two layers. The solution was allowed to stand at room temperature overnight, whereupon well-formed blue crystals suitable for X-ray crystallography were obtained from the dark blue solution. The crystals were filtered and washed with ethanol and diethyl ether and dried in air. Yield 123 mg (95%). FTIR (KBr, cm^{-1}): 3348(vs), 3294(vs), 3233(vs), 3149(vs), 1612(s), 1586(s), 1482(w), 1455(m), 1382(m), 1353(w), 1299(m), 1264(sh), 1088(vs, br), 906(m), 889(s), 879(s), 705(m), 658(m), 624(vs), 587(s), 517(s), 444(m). Anal. calcd for $C_{17}H_{52}Cl_4Cu_6N_8O_{25}$: C, 15.81; H, 4.06; N, 8.68. Found: C, 15.50; H, 3.98; N, 8.83%.

Physical Measurements. IR spectra on powdered samples were recorded with a ThermoNicolet IR200FTIR using KBr pellets. Elemental analyses were performed using a VarioEl III elemental analyzer. Magnetization and variable temperature (2–300 K) magnetic susceptibility measurements on polycrystalline samples were carried out with a Quantum Design SQUID MPMS XL-5 device operating at different magnetic fields. The experimental susceptibilities were corrected for the diamagnetism of the constituent atoms by using Pascal's tables.

X-ray Data Collection and Structure Refinement. Crystallographic data were collected at 123 K for **1**–**8** with a Nonius-Kappa CCD area-detector diffractometer using graphite monochromatized Mo Kα radiation (λ = 0.71073 Å). The data were collected by ϕ and ω rotation scans and processed with the DENZO-SMN ν0.97.638 software package.[17] Empirical absorption corrections were performed with the SADABS program.[18] The structures were solved by direct methods using the SUPERFLIP program,[19] and full-matrix, least-squares refinements on F^2 were performed using the SHELXL-97 program[20] with the WinGX graphical user interface.[21] Thermal ellipsoid plots were obtained by using the DIAMOND program.[22] The partial packing diagrams were drawn with the MERCURY program.[23] All non-hydrogen atoms for complexes **1**–**8** were refined anisotropically. The μ_4-OH hydrogen atom in the structures of **2** and **3**, the OH hydrogen atom of the methanol molecule in the structure of **8**, and the OH hydrogen atoms of Hae molecules in the structures of **4** and **5** were located from the difference Fourier map and were refined isotropically with fixed distances, while other hydrogen atoms were constrained to ride on their parent atoms. In **8**, one carbon atom of the aminoethanolato anion had disorder over two sites (C6A and C6B), and one perchlorate anion had rotational disorder over two sites (O21A, O22A, O23A, O24A and O21B, O22B, O23B, O24B) with relative occupancies refined to 0.59 and 0.41. Restraints were applied to the geometrical and displacement parameters of the disordered perchlorate anion. The crystal data for **1**–**3** and **8** and **4**–**7**, along with other experimental details are summarized in Table 1 and Table S1, Supporting Information, respectively.

Computational Details. All theoretical calculations were carried out at the DFT level of theory using the hybrid B3LYP exchange–correlation functional,[24–26] as implemented in the Gaussian 03 program.[27] A quadratic convergence method was employed in the SCF process.[28] The triple-ζ quality basis set proposed by Ahlrichs and co-workers has been used for all atoms.[29] Calculations were performed on the complexes built from the experimental geometries The electronic configurations used as starting points were created using the Jaguar 7.6 software.[30] The approach used to determine the exchange coupling constants for polynuclear complexes has been described in detail elsewhere.[31–34]

RESULTS AND DISCUSSION

Syntheses. We have earlier reported reactions of Cu(II) ions with Hae and Hap[12f,k–m] and obtained dinuclear and trinuclear Cu(II) complexes. In order to prepare heterometallic Cu(II) amino alcohol complexes, the synthetic part reports the

Table 1. Summary of Crystallographic Data for 1−3 and 8

complex	1	2	3	8
chemical formula	$C_{16}H_{41}Ag_1Cu_4N_8O_{17}$	$C_{16}H_{41}Cu_4N_8Na_1O_{17}$	$C_{16}H_{41}Cu_4K_1N_8O_{17}$	$C_{17}H_{52}Cl_4Cu_6N_8O_{25}$
formula mass	979.60	894.72	910.83	1291.71
crystal system	tetragonal	tetragonal	tetragonal	triclinic
a, Å	13.0938(6)	13.1240(5)	13.1330(4)	10.8965(4)
b, Å	13.0938(6)	13.1240(5)	13.1330(4)	12.1168(3)
c, Å	9.4657(3)	9.4257(2)	9.6551(2)	17.4238(7)
α, deg	90	90	90	92.718(2)
β, deg	90	90	90	107.133(2)
γ, deg	90	90	90	97.842(2)
unit cell volume, Å^3	1622.87(12)	1623.48(9)	1665.27(8)	2168.48(13)
temp, K	123(2)	123(2)	123(2)	123(2)
space group	$P4_2/n$	$P4_2/n$	$P4_2/n$	$P\bar{1}$
no. of formula units per unit cell, *Z*	2	2	2	2
radiation type	Mo K*α*	Mo K*α*	Mo K*α*	Mo K*α*
absorp coeff, *μ*, mm^{-1}	3.253	2.68	2.725	3.227
no. of reflns measured	9956	16294	12284	17730
no. of indep reflns	1593	1593	1626	7587
R_{int}	0.0406	0.0409	0.0397	0.036
final R_1 values ($I > 2\sigma(I)$)[a]	0.0520	0.0522	0.0509	0.0544
final $wR(F^2)$ values ($I > 2\sigma(I)$)[b]	0.0953	0.0989	0.1152	0.117
final R_1 values (all data)	0.0684	0.0611	0.0600	0.0658
final $wR(F^2)$ values (all data)	0.1026	0.1034	0.1209	0.1222
GOF on F^2	1.101	1.043	1.049	1.077

[a] $R_1 = \sum||F_o| - |F_c||/\sum|F_o|$. [b] $wR_2 = \{\sum[w(F_o^2 - F_c^2)^2]/\sum[w(F_o^2)^2]\}^{1/2}$ and $w = 1/[\sigma^2(F_o^2) + (aP)^2 + bP)]$, where $P = (2F_c^2 + F_o^2)/3$.

survey of reactions of $Cu(NO_3)_2{\cdot}3H_2O$ with *N*,*N*-dimethylaminoethanol (Hdmae), 2-aminoethanol (Hae), 3-aminopropanol (Hap), and *N*,*N*-dimethylaminopropanol (Hdmap) and of $Cu(ClO_4)_2{\cdot}6H_2O$ with Hae in the presence or absence of MNO_3 [M = Ag(I), Na(I), or K(I)]. The synthetic routes to the new complexes are presented in Figure 1.

In the synthesis of **1**−**3**, the stoichiometry of the reactants was varied by using stock solutions containing from 0.02 to 0.2 mmol of Cu(II), Ag(I), Na(I), and K(I) nitrates and from 0.04 to 0.48 mmol of Hdmae in 1 mL. For K(I) nitrate stock solutions, a methanol−water 4:1 mixture was used to improve the solubility of KNO_3.

Blue crystals, with some colorless silver and sodium nitrate crystals, were obtained in methanol with copper to silver to Hdmae ratios of 2:1:1.6, 2:1:2.4, and 2:1:4.8 and with copper to sodium to Hdmae ratios of 1:1:2.4, 1:1.2:2.4, and 3.3:1:8. The blue crystals were analyzed by X-ray diffraction and structures of tetranuclear Cu(II) complexes $[Cu_4(\mu_4\text{-}OH)(dmae)_4][Ag(NO_3)_4]$ (**1**) and $[Cu_4(\mu_4\text{-}OH)(dmae)_4][Na(NO_3)_4]$ (**2**) (Figures 2 and 3) were obtained. The reaction's stoichiometry is presented in eq 1:

$$4Cu(NO_3)_2 + MNO_3 + H_2O + 9Hdmae \rightarrow [Cu_4(\mu_4\text{-}OH)(dmae)_4][M(NO_3)_4](s) + 5[H_2dmae]NO_3 \quad (1)$$

During the synthesis of **1** and **2** sodium and silver nitrate crystals were formed with the main product in several cases. This could be avoided if the syntheses were performed in methanol with copper to M(I) to Hdmae ratios of 4:1:9.6. This is a nearly stoichiometric ratio of the reactants.

$[Cu_4(\mu_4\text{-}OH)(dmae)_4][K(NO_3)_4]$ (**3**) was also synthesized in a reaction similar to **1** and **2**, but we were not able to prepare **3** without KNO_3 crystals, although a correct copper to potassium ratio (4:1) and a methanol−water 4:1 mixture as solvent for KNO_3 were used. The methanol−water mixture was used to improve the solubility of potassium nitrate. However, increasing water concentration in the methanol led to the formation of a white precipitate without **3**. Since **3** could not be prepared without KNO_3 crystals, **3** was separated mechanically for the analyses. Due to the small amount of the material, magnetic measurements were not performed for **3**.

The μ_4-hydroxo- and alkoxo-bridged tetranuclear $[Cu_4(\mu_4\text{-}OH)(dmae)_4]^{3+}$ cations are easily formed from copper(II) nitrate and amino alcohols after the deprotonation of the OH groups of the amino alcohol ligands and a water molecule in the excess of amino alcohol acting as a base. In the presence of Ag(I), Na(I), and K(I) nitrate ions, $[M(NO_3)_4]^{3-}$ anions form at least in the solid state with a distorted dodecahedral coordination sphere.

Since we were successful with *N*,*N*-dimethylaminoethanol in the preparation of these tetranuclear complexes, we studied whether 2-aminoethanol, 3-aminopropanol, and *N*,*N*-dimethylaminopropanol could form similar tetranuclear Cu(II) complexes or other polynuclear Cu(II) complexes. In these studies, the stoichiometry of the reactants was also varied by using stock solutions containing in 1 mL of solvent (methanol, ethanol, or acetonitrile) from 0.04 to 0.48 mmol of Hae and Hdmap and from 0.02 to 0.2 mmol of Hae and Hdmap with 0.022 to 0.22 mmol of triethylamine (used as an extra base). For Hap only, a stock solution containing 0.48 mmol of Hap in 1 mL of methanol was used. In addition to the methanol stock solutions used in the synthesis of **1**−**3**, stock solutions containing in 1 mL of solvent (ethanol or acetonitrile) from 0.02 to 0.2 mmol of Cu(II) and Ag(I) nitrates were also used.

The tests using Hae as a chelating agent lead to formation of three new complexes. A known dimeric Cu(II) compound $[Cu(ae)(Hae)]_2(NO_3)_2$[5a] was obtained (AETCUA in CSD) when amounts of materials ($Cu(NO_3)_2{\cdot}3H_2O$, MNO_3 (M = Na, K, or Ag) ,and Hae) equivalent to those in the syntheses of

dx.doi.org/10.1021/ic401325b | *Inorg. Chem.* 2013, 52, 11096−11109

1−**3** were used in methanol. The same dimeric complex was also the main product when the copper to silver to Hae ratio was 1:1:4.8, 1:2:9.6, or 2:1:4.8 and the reaction was performed in methanol, ethanol, or acetonitrile. A few crystals of a new mononuclear $[Cu(Hae)_2(NO_3)_2]$ complex (**4**, Figure S1, Supporting Information) along with the main product, $[Cu(ae)(Hae)]_2(NO_3)_2$, were obtained when the copper to silver to Hae ratio was 2:1:4.8 and the reaction was performed in acetonitrile. A few crystals of a new tetranuclear heterometallic $[Ag_2Cu_2(ae)_2(Hae)_2(NO_3)_4]$ complex (**5**, Figure 4) with $[Cu(ae)(Hae)]_2(NO_3)_2$ were obtained in the synthesis where the copper to silver to Hae ratio was 2:1:4.8 and the reaction was performed in methanol. When the copper to silver to Hae ratios were 1:1:4 and 1:1:4.8 and ethanol was used as solvent, a few faintly red shaded crystals of a new silver(I)/copper(I) oxazino-oxazine $[Ag_{0.93}Cu_{0.07}(C_6H_{12}N_2O_2)NO_3]$ complex (**6**, Figure 5) were obtained along with the main product $[Cu(ae)(Hae)]_2(NO_3)_2$. When the copper to silver to Hae ratio was 1:2:4.8 or 1:1:2.4 and triethylamine was used as base, and the reaction was performed in methanol, the previously reported[12m] trinuclear copper(II) $[Cu_3(ae)_4(NO_3)_2]$ complex was obtained as the sole product, while $[Cu(ae)(Hae)]_2(NO_3)_2$ was obtained when the reaction was performed in ethanol or acetonitrile. No tetranuclear Cu(II) units were obtained with Hae although the reactions were performed in a way similar to those for **1**−**3** in presence of copper(II) nitrate and $M(NO_3)$, but compounds $[Cu(ae)(Hae)]_2(NO_3)_2$ and **4**−**6** were formed instead.

A known dinuclear copper(II) $[Cu_2(ap)_2(NO_3)_2]$[12f,k] complex was obtained when amounts of materials (Cu(II) nitrate, MNO_3 (M = Na, K, or Ag), and Hap) equivalent to those in the syntheses of **1**−**3** were used in methanol. This dinuclear copper(II) complex was the sole product whenever silver, sodium, or potassium nitrate was used in the synthesis.

A new polymeric dinuclear copper(II) $[Cu_2(dmap)_2(NO_3)_2]$ complex (**7**, Figure 6) was obtained when amounts of materials ($Cu(NO_3)_2{\cdot}3H_2O$, MNO_3 (M = Na or Ag), and Hdmap) equivalent to those in the syntheses of **1** and **2** were used in methanol. The synthesis of the new dinuclear copper(II) complex **7** was further studied with copper nitrate using only Hdmap or Hdmap with triethylamine as a base. The dinuclear complex **7** was obtained with both methods using methanol or ethanol as solvent. The new complex **7** was not formed when acetonitrile was used as solvent. Although none of the tested three amino alcohols formed similar copper(II) nitrate complexes as Hdmae did, three new copper(II) complexes and one silver(I) complex were obtained in the syntheses performed.

To obtain some insight into the role of the anion, we performed some tests with Hae in which we used copper(II) perchlorate instead of copper(II) nitrate as a copper source. When the amounts of copper(II) perchlorate and ae^- (ae^- from Hae with $N(Et)_3$) were varied from 1:1 to 1:3 in methanol, the hexanuclear "bicapped cubane" complex $[Cu_6(ae)_8(ClO_4)_2](ClO_4)_2{\cdot}MeOH$ (**8**) (Figures 7 and 8) was always formed in a good yield.

This work reveals that the amino alcohols with slightly different molecular structures can form copper(II) complexes with a large structural diversity from mononuclear copper(II) units to several different polynuclear units. A labile copper(II) ion quickly reacts with the ligands. Thus the thermodynamic control dominates the formation of the complexes. Crystal packing forces are important in a formation of these complexes. Different complexes can be achieved by variation of the stoichiometry of copper(II) ions, amino alcohols, and other metal ions. The solvents and anions used may play an important role in the formation of certain complexes.

Description of the Structures. The crystal structures of complexes **1**−**3** consist of almost planar tetranuclear $[Cu_4(\mu_4\text{-}OH)(dmae)_4]^{3+}$ units, in which the Cu(II) ions are also weakly bonded to the nitrate anions. The adjacent tetranuclear units in **1**−**3** are connected by ionic interactions through nitrate anions of anionic silver, sodium, or potassium complexes resulting in the formation of 1D polymeric pillars. The crystal structure of **8** consists of hexanuclear $[Cu_6(ae)_8]^{4+}$ "bicapped cubane" units, in which the capping Cu(II) ions are weakly bonded to perchlorate anions. The adjacent hexanuclear units of **8** are connected by hydrogen bonds resulting in the formation of 3D hydrogen bonded networks. The corresponding tetranuclear and hexanuclear units, the tetranuclear and hexanuclear cores, and the atom numbering schemes for **2** and **8** are shown in Figures 2 and 3 and 7 and 8, respectively. Selected bond and

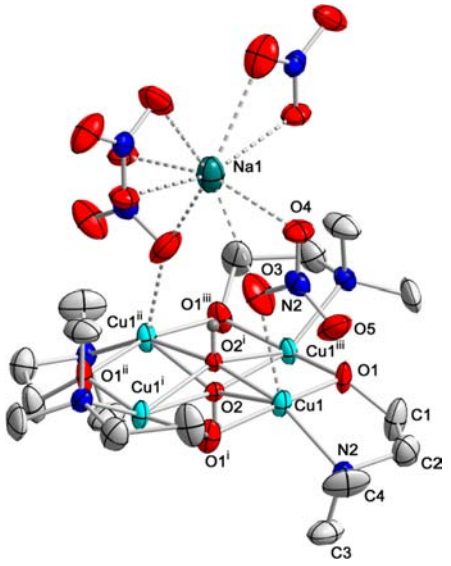

Figure 2. The tetranuclear cation $[Cu_4(\mu_4\text{-}OH)(dmae)_4]^{3+}$ and $[Na(NO_3)_4]^{3-}$ anion connected by the bridging nitrates in **2** showing the atomic labeling scheme with thermal ellipsoids drawn at the 30% probability level. The hydrogen atoms are omitted for clarity. Symmetry codes: (i) $-x + 3/2, y, -z + 1/2$; (ii) $-x + 3/2, -y + 3/2, z$; (iii) $x, -y + 3/2, -z + 1/2$.

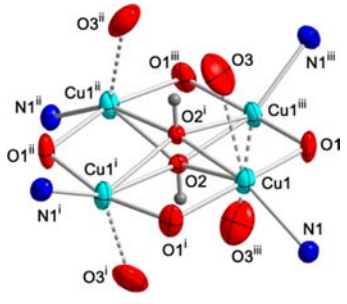

Figure 3. The tetranuclear μ_4-OH bridged core of **2** with the coordination environment of the copper(II) centers drawn at the 30% probability level. Symmetry codes as in Figure 2

dx.doi.org/10.1021/ic401325b | Inorg. Chem. 2013, 52, 11096−11109

hydrogen bond parameters for **1**−**3** are presented in Table 2 and Table S2, Supporting Information, and for **8** in Table 3 and Table S3, Supporting Information. The additional structures of complexes **4**−**7** are presented in Figure S1, Supporting Information, and Figures 4−6, respectively, and are briefly discussed. The bond and hydrogen bond parameters for **4**−**7** are presented in Tables S4−S10, Supporting Information.

Table 2. Selected Bond Lengths (Å) and Angles (deg) for 1−3[a]

	1	2	3
Cu1···Cu1^{i}	2.9472(12)	2.9485(12)	2.9621(11)
Cu1···Cu1^{ii}	4.152(2)	4.149(2)	4.1757(15)
Cu1−O1	1.910(5)	1.915(5)	1.917(5)
Cu1−O1^{i}	1.909(5)	1.913(5)	1.912(5)
Cu1−O2	2.131(3)	2.133(3)	2.147 (3)
Cu1−O2^{i}	2.0873(15)	2.0847(13)	2.1043(15)
Cu1−O3	2.418(8)	2.401(9)	2.363(7)
Cu1···O5	2.647(9)	2.710(9)	2.640(7)
Cu1−N1	2.002(6)	2.010(6)	2.017(6)
M−O3[b]	2.694(9)	2.678(9)	2.879(8)
M−O4[b]	2.672(6)	2.583(5)	2.888(6)
Cu1···O1$_4$ plane	0.131	0.146	0.118
O2··· O1$_4$ plane	0.350	0.351	0.381
Cu1−O1−Cu1^{iii} (θ)	101.0(2)	100.7(3)	101.4(3)
Cu1−O2−Cu1^{iii} (θ)	88.64(10)	88.69(8)	88.34(9)
Cu1−O2^{i}−Cu1^{ii} (θ)	168.0(7)	168.7(6)	165.7(6)
Cu1 (δ)[c]	0.227	0.189	0.243
O2^{i}···O1−C1 (τ)[d]	33.9(7)	32.1 (7)	33.0 (6)
Cu1−O1−O2−Cu1^{iii} (γ)[e]	12.1(5)	12.1(4)	13.1(4)
Cu1−O1−O2^{i}−Cu1^{iii} (γ)[e]	12.1(5)	12.3(4)	13.0(4)
O1−O1^{i}−O1^{ii}−O1^{iii}	0.0(4)	0.1(4)	0.1(3)
Cu1−Cu1^{i} (ω)[f]	20.8(2)	19.1(2)	22.6(2)
Cu1−Cu1^{iii} (ω)[f]	21.4 (2)	19.6(2)	23.2 (2)
Cu1−Cu1^{ii} (ω)[f] (O2)	18.29(13)	15.63(10)	20.06(13)
Cu1−Cu1^{ii} (ω)[f] (O2^{i})	38.2(2)	35.50(13)	41.45(15)

[a]Symmetry codes: (i) $-x + 3/2, y, -z + 1/2$; (ii) $-x + 3/2, -y + 3/2, z$; (iii) $x, -y + 3/2, -z + 1/2$. [b]M for **1**, Ag1; for **2**, Na1; for **3**, K1. [c]The distortion of the coordination geometry for five-coordinated complexes is $\delta = (\alpha - \beta)/60$ (α and β are the larger *trans* X−Cu−X angles, δ is 1 for a trigonal-bipyramidal geometry and 0 for a square pyramid).[35] [d]τ is the substituents angle from the bridging O···O line. [e]γ is the dihedral angle of the bridging O−Cu−O planes. [f]ω is the dihedral angle between the coordination planes of Cu(II) ions.

*[Cu$_4$(μ_4-OH)(dmae)$_4$][Na(NO$_3$)$_4$] (**2**).* The tetranuclear complexes **1**−**3** crystallize in the tetragonal space group $P4_2/n$. Complexes **1**−**3** are isostructural with only small differences in the equivalent bond lengths and angles (Table 2). Therefore the structure of **2** is discussed here and compared with structures of **1** and **3** only where notable differences occur. The asymmetric unit of **2** consists of one [Cu(dmae)]$^+$ unit, one nitrate anion, and one-fourth of both a hydroxide anion and a sodium cation. The tetranuclear copper(II) core of **2** consists of four [Cu(dmae)]$^+$ units connected by the O2 oxygen atom of the central μ_4-OH anion. The four copper atoms are not coplanar; the adjacent copper atoms are 0.146 Å above and below the square plane formed by alkoxo oxygen atoms, O1. The copper atoms have distorted (4 + 1) square pyramidal coordination spheres (see δ parameters in Table 2). Each of the four copper(II) atoms is coordinated by two alkoxide oxygen atoms forming an additional μ_2-O bridge between adjacent copper atoms, with Cu−O distances of 1.915(5) and 1.913(5) Å, a central hydroxide oxygen atom with Cu−O distances of 2.133(3) and 2.0847(13) Å, and one amine nitrogen atom with a Cu−N distance of 2.010(6) Å in the equatorial plane. The axial coordination site is occupied by an oxygen atom of the nitrate anion with a Cu−O distance of 2.401(9) Å. The central μ_4-OH anion lies on a crystallographic S_4 axis, is disordered over two sites due symmetry, and is 0.351 Å above and below the plane by alkoxo O1 atoms (center of the cavity). The disorder of the central O2 atom is further displaced in the elongation of its thermal ellipsoids in the direction of the S_4 axis. The hydrogen atom of the central μ_4-OH anion in complexes **2** and **3** could be refined but not that for **1**, and thus its position in **1** was calculated.

The Cu1−O−Cu1^{iii} bridging angles (θ) around O1 and O2 are 100.7(3)° and 88.69(8)°, respectively. The bridging Cu1(μ-O)$_2$Cu1^{iii} fragment is slightly folded with Cu1−O1−O2−Cu1^{iii} and Cu1−O1−O2^{i}−Cu1^{iii} angles (γ) of 12.1(4)° and 12.3(4)°. The τ angle (the substituent angle with respect to the bridging O···O line), as defined by Ruiz et al.[13c] is 32.1(7)° for O2^{i}−O1−C1. The relatively small average of θ angles, large τ angle, and slight folding of the Cu1(μ-O)$_2$Cu1^{iii} bridging fragment, as found in our previous studies for trinuclear linear alkoxo-bridged copper(II) complexes,[12m] results in the shortening of the Cu···Cu separation leading to a Cu1···Cu1^{i} distance of 2.9485(12) Å. The sodium cation in the structure of **2** has a dodecahedral coordination environment and is surrounded by eight nitrate oxygen atoms with Na−O distances of 2.678(9) and 2.583(9) Å. These M−O (M = Ag, Na, or K) distances in the structures of **1**−**3** become longer as the ionic radii of the metal cation increase, leading also to the elongation of the *c*-axis of the unit cell. The adjacent tetranuclear [Cu$_4$(μ_4-OH)-(dmae)$_4$]$^{3+}$ cations of **1**−**3** are connected by O3 and O4 oxygen atoms of the nitrate anion to [M(NO$_3$)$_4$]$^{3-}$ anions (Ag(I) in **1**, Na(I) in **2**, and K(I) in **3**) resulting in the formation of pillar-like 1D polymer chains along the (001) plane (Figure S2, Supporting Information).

*Complexes **4**−**7**.* The structure of **4** is presented in Figure S1, Supporting Information, with selected bond parameters in Table S4, Supporting Information. The chelating neutral Hae ligands adopt the *trans*-arrangement, and Cu(II) has an elongated octahedral coordination sphere. The axial coordination sites of the copper atom are occupied by the oxygen atoms of the nitrate anions. The adjacent mononuclear [Cu-(Hae)$_2$(NO$_3$)$_2$] units are connected by hydrogen bonds (Table S5, Supporting Information). This is the first example of a mononuclear Cu(II) complex with neutral amino alcohols and small nitrate anions.

The structure of tetranuclear heterometallic Cu(II)/Ag(I) complex **5** is presented in Figure 4 with selected bond parameters in in Table S6. The distorted square pyramidal coordination sphere of the copper(II) ions consists of two alkoxide oxygen atoms and two amine nitrogen atoms in a plane and an axial coordination site is occupied by an oxygen atom of the neutral Hae, which also forms a bridge to the Ag(I) ion. The silver atoms are also connected to the Cu(μ-O)$_2$Cu-core by alkoxide oxygen atoms, which act as μ_3−O bridging ligands. The coordination sphere of the Ag(I) is completed by the oxygen atoms of the monodentate and the bidentate nitrate anion. The adjacent tetranuclear [Ag$_2$Cu$_2$(ae)$_2$(Hae)$_2$(NO$_3$)$_2$] units are connected to each other by hydrogen bonds (Table S7).

The silver(I) oxazino-oxazine [Ag(C$_6$H$_{12}$N$_2$O$_2$)NO$_3$] complex **6** (Figure 5 and Table S8, Supporting Information)

dx.doi.org/10.1021/ic401325b | *Inorg. Chem.* 2013, 52, 11096−11109

Table 3. Selected Bond Lengths (Å) and Angles (deg) for 8

Cu1−O1	1.982(4)	Cu2−O1	2.015(5)
Cu1−O2	1.999(5)	Cu2−O2	1.966(4)
Cu1−O4	2.209(5)	Cu2−O3	2.215(5)
Cu1−O5	1.897(5)	Cu2−O7	1.899(5)
Cu1−N1	2.002(6)	Cu2−N2	2.021(7)
Cu3−O2	2.117(5)	Cu4−O1	2.033(5)
Cu3−O3	1.960(5)	Cu4−O3	2.198(5)
Cu3−O4	2.139(5)	Cu4−O4	1.949(4)
Cu3−O6	1.930(5)	Cu4−O8	1.916(5)
Cu3−N3	1.982(7)	Cu4−N4	1.993(6)
Cu5−O5	1.935(5)	Cu6−O7	1.944(5)
Cu5−O6	1.961(5)	Cu6−O8	1.939(5)
Cu5−N5	2.018(6)	Cu6−N7	1.991(6)
Cu5−N6	1.996(6)	Cu6−N8	2.012(6)
Cu5···O9	2.798(6)	Cu6···O13	2.619(5)
Cu1···Cu2	2.9940(10)	Cu2···Cu3	3.1617(11)
Cu1···Cu3	3.1057(11)	Cu2···Cu4	3.1324(11)
Cu1···Cu4	3.1001(11)	Cu3···Cu4	3.0770(11)
Cu1···Cu5	3.4878(10)	Cu2···Cu6	3.4173(10)
Cu3···Cu5	3.5543(10)	Cu4···Cu6	3.4676(10)
Cu1−O1−Cu2 (θ)	97.0(2)	Cu2−O2−Cu3 (θ)	101.5(2)
Cu1−O2−Cu2 (θ)	98.1(2)	Cu2−O3−Cu3 (θ)	98.3(2)
Cu1−O2−Cu3 (θ)	97.9(2)	Cu2−O1−Cu4 (θ)	101.4(2)
Cu1−O4−Cu3 (θ)	91.2(2)	Cu2−O3−Cu4 (θ)	90.4(2)
Cu1−O1−Cu4 (θ)	101.1(2)	Cu3−O3−Cu4 (θ)	95.3(2)
Cu1−O4−Cu4 (θ)	96.2(2)	Cu3−O4−Cu4 (θ)	97.5(2)
Cu1−O5−Cu5 (θ)	131.1(3)	Cu2−O7−Cu6 (θ)	125.6(3)
Cu3−O6−Cu5 (θ)	132.0(3)	Cu4−O8−Cu6 (θ)	128.2(3)
Cu1 (δ)[a]	0.337	Cu2 (δ)	0.284
Cu3 (δ)	0.520	Cu4 (δ)	0.343
Cu5 (δ)	0.037	Cu6 (δ)	0.028
O2···O1−C1 (τ)[b]	35.7(4)	O1···O2−C3 (τ)	35.8(4)
O4···O3−C5 (τ)	41.6(5)	O3···O4−C7 (τ)	44.0(4)
Cu1−O1−O2−Cu2 (γ)[c]	16.0(3)	Cu2−O2−O3−Cu3 (γ)	4.0(3)
Cu1−O2−O4−Cu3 (γ)	15.0(2)	Cu2−O1−O3−Cu4 (γ)	13.9(2)
Cu1−O1−O4−Cu4 (γ)	6.1(3)	Cu3−O3−O4−Cu4 (γ)	5.1(3)

[a]The distortion of the coordination geometry for five-coordinated complexes is $\delta = (\alpha - \beta)/60$ (α and β are the larger *trans* X−Cu−X angles, δ is 1 for a trigonal-bipyramidal geometry and 0 for a square pyramid).[35] [b]τ is the substituents angle from the bridging O···O line. [c]γ is the dihedral angle of the bridging O−Cu−O planes.

consists of one silver(I) ion, one oxazino-oxazine molecule, and one nitrate anion. An oxygen atom of the nitrate anion and two nitrogen atoms of the adjacent oxazino-oxazine ligands are coordinated to one silver(I) ion forming 1D polymeric chains, which are further connected to each other through hydrogen bonds (Table S9, Supporting Information). This intriguing oxazino-oxazine ligand is formed by a condensation reaction of the three aminoethanol molecules by releasing one water and one ammonia molecule with unknown mechanism in the presence of Cu(II) and Ag(I) ions. Tests using only silver(I) or copper(II) ions were not successful. The refinement also suggested that there is a small amount (7%) of Cu(I) cations in the crystal.

The centrosymmetric dinuclear complex **7** consists of the dinuclear $[Cu_2(dmap)_2]^{2+}$ units and two nitrate anions (Figure 6 and Table S10, Supporting Information). The coordination sphere of copper(II) ions consists of two alkoxide oxygen atoms, one amine nitrogen atom, and one oxygen atom from the nitrate anion. The fifth coordination site of copper atoms is occupied by an oxygen atom of the nitrate anion from the adjacent dinuclear unit at 2.732(2) Å. This nitrate oxygen atom acts as a bridge between adjacent dinuclear units leading to the formation of 1D polymeric chains.

$[Cu_6(ae)_8(ClO_4)_2](ClO_4)_2$·MeOH (**8**). The hexanuclear "bicapped cubane" complex **8** crystallizes in the triclinic space group $P\bar{1}$. The asymmetric unit of **8** (Figure 7) consists of one $[Cu_6(ae)_8]^{4+}$ unit, four perchlorate anions and one methanol molecule. The hexanuclear copper(II) core is presented in Figure 8, showing the top and bottom faces of the cubane Cu_4ae_4 subcore capped by two copper atoms, Cu5 and Cu6. The two capping copper atoms are joined via alkoxo oxygen bridges to the two copper atoms on the top and bottom faces of the cubane Cu_4ae_4 subcore. The copper atoms Cu1, Cu2, and Cu4 of the cubane subcore have distorted (4 + 1) square pyramidal coordination spheres, whereas the copper atom Cu3 of the cubane subcore has a (4 + 1) coordination sphere intermediate between square pyramidal and trigonal bipyramidal coordination (see δ parameters in Table 3). The capping copper atoms, Cu5 and Cu6, have (4 + 1) square pyramidal coordination spheres (see δ parameters in Table 3). The Cu···Cu distances within the cubane subcore are between 2.9940(10) and 3.1617(11) Å, and for the capping and cubane

dx.doi.org/10.1021/ic401325b | Inorg. Chem. 2013, 52, 11096−11109

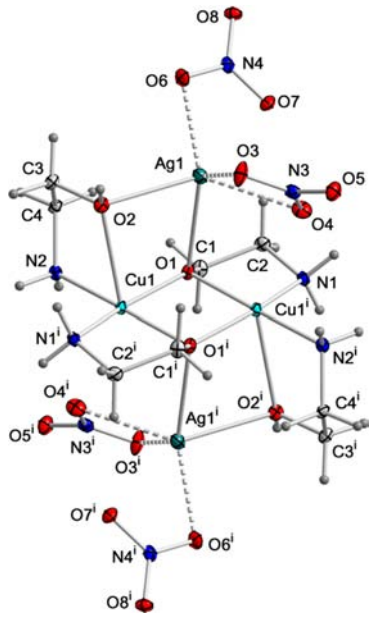

Figure 4. The structure of **5** showing the atomic labeling scheme with thermal ellipsoids drawn at the 30% probability level. Symmetry code: (i) $-x + 1/2, -y + 1/2, -z$.

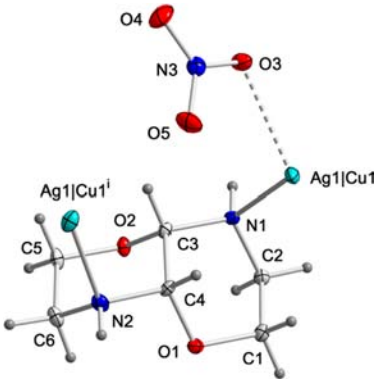

Figure 5. The structure of **6** showing the atomic labeling scheme with thermal ellipsoids drawn at the 30% probability level. Symmetry code: (i) $x, -y + 1/2, z - 1/2$.

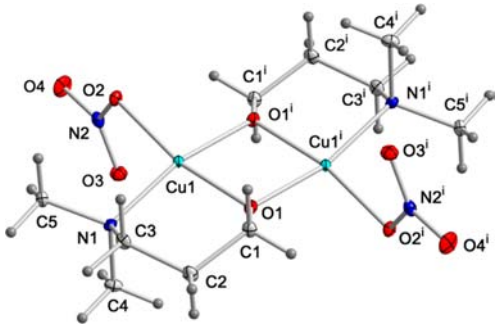

Figure 6. The structure of **7** showing the atomic labeling scheme, with thermal ellipsoids drawn at the 30% probability level. Symmetry code: (i) $-x + 1, -y, -z$.

copper atoms, the Cu···Cu distances are between 3.4173(10) and 3.5543(10) Å. All four copper(II) atoms of the cubane subcore are coordinated by four alkoxide oxygen atoms forming μ_3-O bridges between adjacent copper atoms, with Cu−O bonds between 1.897(5) and 2.215(5) Å, and one amine nitrogen atom, with Cu−N bonds between 1.982(7) and 2.021(7) Å. The two capping copper(II) atoms are coordinated by two alkoxide oxygen atoms forming μ_2-O bridges between adjacent copper atoms with Cu−O bond between 1.935(5) and 1.961(5) Å, and two amine nitrogen atoms with Cu−N bonds between 1.991(6) and 2.018(6) Å in the equatorial plane. The axial coordination sites of the two capping copper Cu5 and Cu6 atoms are occupied by oxygen atoms of perchlorate anions with a Cu5−O9 and Cu6−O13 distances of 2.798(6) and 2.619(5) Å, respectively. The Cu−O−Cu bridging angles (θ) of the cubane core are between 90.4(2)° and 101.5(2)°, the two smallest angles being in the top and bottom faces of the cubane core. The θ bridging angles between the capping and cubane copper atoms are substantially larger, between 125.6(3)° and 132.0(3)°. The bridging Cu(μ-O)$_2$Cu fragments are slightly folded with Cu−O−O−Cu angles (γ) from 4.0(3)° to 16.0(3)°. The τ angles are between 35.7(4)° and 44.0(4)°. The adjacent hexanuclear $[Cu_6(ae)_8(ClO_4)_2](ClO_4)_2$·MeOH units are connected by hydrogen bonds (Table S3, Supporting Information) involving the NH hydrogen atoms, hydrogen and oxygen atoms of the methanol molecule, and perchlorate oxygen atoms, resulting in the formation of a 3D hydrogen bonded network (Figure S3, Supporting Information).

Magnetic Properties. A magnetostructural study of **1** and **2** is of interest since, as far as we know, only a few μ_4-(OH) bridged tetranuclear copper(II) complexes have been reported in the literature,[15] and the magnetic properties of only one of them were studied.[15c] The temperature dependence of χ_M and $\chi_M T$ (χ_M is the molar magnetic susceptibility per Cu_4 unit) for **1** and **2** in the range 300−2 K and at an applied field of 1000 Oe is shown in Figure 9.

The $\chi_M T$ value at room temperature (1.64 $cm^3\ mol^{-1}K$) is close to that expected for four uncoupled Cu^{2+} ions ($S = 1/2$) with $g = 2.0$ (1.50 $cm^3\ mol^{-1}$ K). The $\chi_M T$ decreases with decreasing temperature, first slightly until ∼100 K and then sharply to reach a value close to zero at 2 K. This behavior suggests the existence of a moderate global antiferromagnetic interaction in both compounds. The presence of a maximum in the χ_M versus T plots (at 24 K for **1** and 30 K for **2**) supports the global antiferromagnetic interaction in these compounds leading to an $S = 0$ singlet ground state. Complex **2** shows an increase in the χ_M versus T below 6 K, which is due to the presence of a small amount of paramagnetic impurity. Due to the S_4 structure of **1** and **2**, the magnetic susceptibility data were fitted to a spin Hamiltonian where the first term (J) accounts for the equivalent magnetic pathways through the sides of the almost square planar Cu_4O_4 moiety, and the second term (J') takes into account the magnetic pathways trough the two diagonals (Scheme 1), according to the following equation:

$$\mathbf{H} = -J(S_{Cu1}S_{Cu2} + S_{Cu2}S_{Cu3} + S_{Cu3}S_{Cu4} + S_{Cu1}S_{Cu4}) - J'(S_{Cu1}S_{Cu3} + S_{Cu2}S_{Cu4})$$

The Hamiltonian was numerically diagonalized using the MAGPACK program.[36] In order to avoid overparametrization, an average g value was assumed for the whole pentanuclear unit. A parameter (ρ) was included to account for the paramagnetic impurity. The best fit parameters were $J = +1.8$ cm^{-1}, $J' = -29.2$ cm^{-1}, $g = 2.10$, and $\rho = 0.026\%$ for **1** ($R = 2.1 \times 10^{-5}$) and $J = +2.9$ cm^{-1}, $J' = -32.2$ cm^{-1}, $g = 2.10$, and $\rho = 0\%$ for **2** ($R = 3.1 \times 10^{-5}$). Poorer but similar quality fits were obtained for small negative J values.

dx.doi.org/10.1021/ic401325b | Inorg. Chem. 2013, 52, 11096−11109

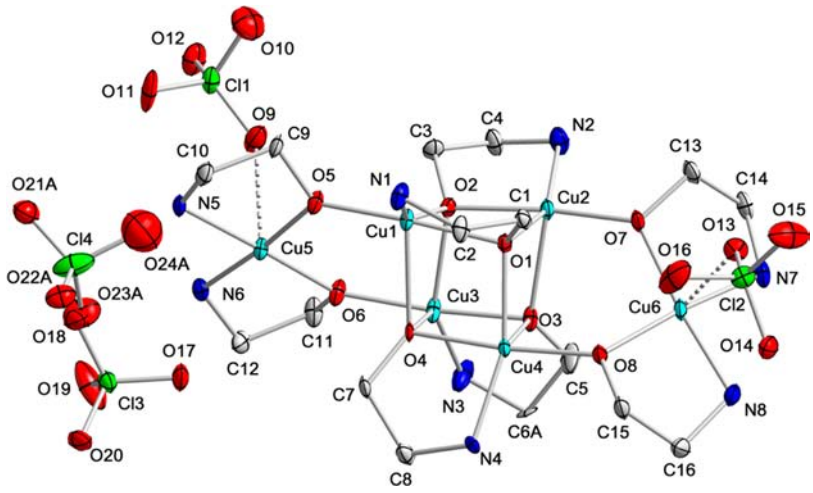

Figure 7. The hexanuclear unit of **8** showing the atomic labeling scheme with thermal ellipsoids drawn at the 30% probability level. The methanol molecule, hydrogen atoms, minor-occupancy carbon site (C6B) of the disordered aminoethanolate anion, and oxygen sites (O21B, O22B, O23B and O24B) of the disordered perchlorate anion are omitted for clarity.

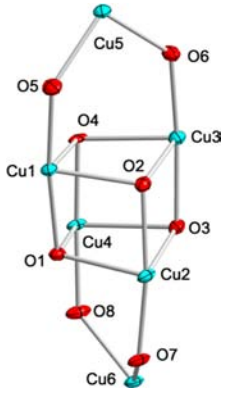

Figure 8. The hexanuclear core of **8** with thermal ellipsoids drawn at the 30% probability level.

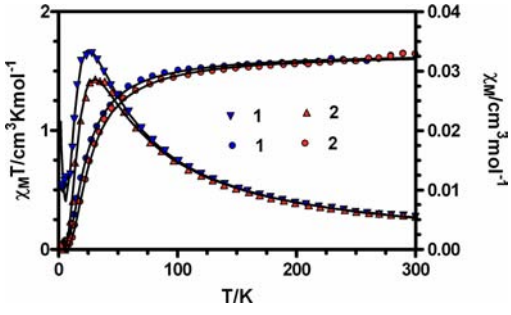

Figure 9. Temperature dependence of the χ_M and $\chi_M T$ for complexes **1** and **2**. Solid lines represent the best fit with the Hamiltonians discussed below.

Both experimental[12] and theoretical[13] studies have shown that the major factor controlling the magnetic exchange interaction in hydroxo- and alkoxo-bridged polynuclear copper(II) complexes is the value of the Cu−O−Cu angle (θ) and an almost linear variation of J with θ has been established for dinuclear complexes, the crossing point between antiferromagnetic and ferromagnetic interactions being located at ∼98°.[12b] DFT calculations carried out on dihydroxo- and dialkoxo-bridged model structures containing a planar $Cu_2(\mu\text{-}O_2)$ skeleton predicted antiferromagnetic interactions for Cu−O−Cu angles (θ) larger than 92° when the τ angle (out-of-plane displacement of the methyl carbon atom from the Cu_2O_2 plane) was zero. Dihydroxo and dialkoxo complexes exhibited antiferromagnetic interactions for the whole range of the Cu−O−Cu angle (θ) when the τ angles were smaller than 40°.[13c,d] Moreover, a correlation was established between θ and τ, showing that small values of θ are associated with the largest values of τ. Therefore, the AF coupling is favored when θ increases and τ diminishes. Besides these two angles, other structural factors, such as the dihedral angle of the O−Cu−O bridging planes (γ), the deviation of the copper(II) coordination geometry from square-pyramidal or square-planar (δ), and the dihedral angle between the coordination planes of the Cu(II) atoms (ω), can also affect the magnitude of the magnetic exchange interaction.[13f] The increase of γ, δ, and ω is expected to reduce the value of the antiferromagnetic exchange interaction. Our recent experimental and theoretical study for bis(μ-alkoxo-bridged) linear trinuclear complexes[12m] and DFT calculations on planar bis(μ-dihydroxo-bridged) trinuclear complexes[13h] showed very similar trends to those found for dinuclear dihydroxo- and dialkoxo-bridged complexes.

Complexes **1** and **2** are isostructural with only small differences in the equivalent bond lengths and angles, and therefore the J and J' values obtained are similar for **1** and **2**. In principle, a weak ferro- or antiferromagnetic interaction would be expected between adjacent copper(II) atoms along the side, as the two bridges connecting these atoms, of the hydroxo/alkoxo type and with Cu1−OH−Cu2 and Cu−O−Cu angles (θ) of 88.64(10)° and 101.0(2)° for **1** and 88.69(8)° and 100.7(3)° for **2**, may counterbalance their effects (F interaction for the former bridge and AF for the latter). Nevertheless, the fact that the dmae$^-$ ligand can increase the τ values (above 30°) and the Cu(μ-O_2)Cu bridging fragment is slightly folded with γ values of 12.1(4)−12.3(4)°, favors the ferromagnetic interactions along the side of the almost square-planar Cu_4O_4 fragment, which is in good agreement with the experimental results.

From the magnetostructural point of view, polynuclear copper complexes with a single hydroxo-bridge are still rare. For the simple dicopper complexes, antiferromagnetic exchange couplings have been observed in all cases with the antiferromagnetic exchange coupling increasing with the Cu−

dx.doi.org/10.1021/ic401325b | Inorg. Chem. 2013, 52, 11096−11109

O−Cu angle.[37,38] Indeed, the σ overlap of the magnetic orbitals of the copper atoms and the p orbital of the hydroxo-bridge increases with the Cu−O−Cu angles closer to 180°. In the view of this, an antiferromagnetic exchange interaction would be expected for the interaction between copper(II) atoms along the diagonal, which is in accordance with the experimental results. It is noteworthy that the J' parameter is lower than those usually found for other monohydroxo-bridged copper complexes with similar Cu1−OH−Cu3 angles (168.0(7)° for **1** and 168.7(6)° for **2**), which could be because (i) the CuO_4N coordination polyhedron exhibits a distorted geometry from square-pyramidal toward trigonal-bipyramidal with an Addison's parameter of ∼0.2 (this parameter is 0 for the former and 1 for the latter). For this distorted geometry, the overlap between the magnetic orbitals (an admixture of $d_{x^2-y^2}$ and d_{z^2}) decreases compared with the case of the square pyramidal geometry where the magnetic orbital is $d_{x^2-y^2}$, and therefore the AF magnetic exchange interaction decreases and (ii) the long Cu···Cu separations of 4.152(2) and 4.149(2) Å for **1** and **2**, respectively, also decrease the overlap between the magnetic orbitals.

In order to support the sign and magnitude of the J and J' exchange coupling parameters observed for **1** and **2**, we have performed DFT calculations on the structure of **2** as found in the solid state and for one of the disordered configurations. The calculated values of the exchange coupling could not be obtained for **1** because of the presence of the silver(I) cation. The calculated J values for **2** are given in the following Scheme 2.

Scheme 2. Calculated J Values for the Broken-Symmetry Model Structure of 2

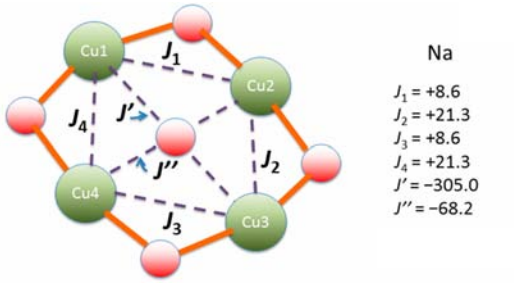

As can be observed, the sign and relative magnitude of these interactions are in a reasonably good accord with the experimental results. It should be noted that this type of DFT calculation correctly predicts the sign of the magnetic interactions but discrepancies usually exist between the magnitude of the experimental and calculated values. This fact may be due to the inherent limitations of the method and to the flexibility of the structure that allows some structural changes when the sample is cooled. To additionally support the sign of the side and diagonal interactions, we have carried out DFT calculations for dinuclear model compounds of the side and diagonal interactions (Figure S4, Supporting Information); the results confirm that the edge interactions are ferromagnetic, whereas the diagonal interactions are antiferromagnetic.

The magnetic properties of **8** in the form $\chi_M T$ versus T (χ_M is the molar magnetic susceptibility per Cu_6 unit), measured in the 300−2 K range and in an applied field of 1000 Oe, are shown in Figure 10. The value of $\chi_M T$ at room temperature, 1.32 $cm^3\ mol^{-1}$ K, is significantly smaller than that expected for

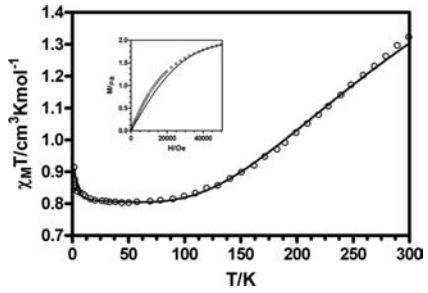

Figure 10. Fitting of the magnetic data of **8** to a model composed of two interacting isosceles triangles and the observed field dependence of the magnetization (inset).

six magnetically isolated copper(II) atoms, 2.25 $cm^3\ mol^{-1}$ K (with S = 1/2 and g = 2), thus indicating a global dominant strong antiferromagnetic coupling between the copper(II) ions. Upon lowering the temperature, $\chi_M T$ further decreases to reach a quasi-plateau at 75 K with a value of ∼0.8 $cm^3\ mol^{-1}$ K, which matches that expected for two S = 1/2 doublets. Below 10 K, $\chi_M T$ increases sharply to reach a value of 0.91 $cm^3\ mol^{-1}$ K at 2 K. The field dependence of the magnetization is given in the inset of Figure 11. The magnetization value at the maximum

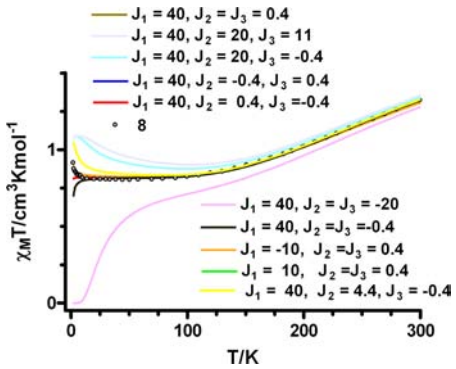

Figure 11. Simulated $\chi_M T$ vs. T curves with the above Hamiltonian.

applied field (1.9μ_B) is close to the saturation value expected for an S = 1 ground state (2.0μ_B with g = 2). The M versus H curve is above the theoretical Brillouin function for two isolated S =1/2 states but below the Brillouin curve expected for an S = 1 state.

This compound contains a very complicated "bicapped cubane" Cu_6O_8 core (Scheme 3). Complexes with this structure are limited to two examples, which were magnetostructurally studied.[9c,16] Interestingly, these compounds exhibit dominant antiferromagnetic interactions leading to an S = 0 ground state. This is an important difference with compound **8**, which also exhibits a dominant antiferromagnetic interaction but with an S = 1 ground state.

A close inspection of the structure of **8** reveals the following magnetostructural features: (i) Although there are eight different magnetic pathways, we are going to assume for the sake of simplicity that some of them are equal. (ii) There exist large Cu−O−Cu angles with an average value of 129.2° (Table 4) involving the capping Cu5 and Cu6 atoms and the cubane copper atoms Cu1 and Cu3 and Cu2 and Cu4 with short Cu−O distances in the range 1.897−1.962 Å. These structural parameters favor a strong antiferromagnetic interaction between the copper(II) atoms. These magnetic pathways are assumed to be described by the same exchange coupling

dx.doi.org/10.1021/ic401325b | Inorg. Chem. 2013, 52, 11096−11109

Scheme 3. Perspective View of the Bicapped Cubane Cu_6O_8 Core of 8 and the Coupling Constants for the Different Magnetic Exchange Pathways[a]

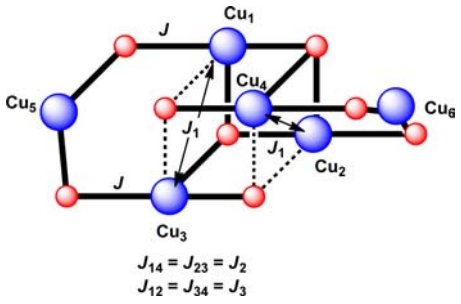

[a]Solid lines and dotted lines represent short distances (Cu–equatorial distances) and long distances (Cu–apical distances), respectively.

Table 4. Structural Parameters and Experimentally Obtained *J* Values for 1, 2, and 8

	1	2	8
Cu···Cu	2.9472(12)[a]	2.9485(12)[a]	3.0952[c]
	4.152(2)[b]	4.149(2)[b]	3.4818[d]
Cu–O–Cu θ (deg)	101.0(2)	100.7(3)	95.2[e]
			98.1[f]
			129.2[g]
Cu1–OH–Cu2 θ (deg)	88.64(10)	88.69(8)	
Cu1–OH–Cu3 θ (deg)	168.0(7)	168.7(6)	
Cu2–OH–Cu4 θ (deg)	153.9(7)	153.1(5)	
Cu δ[h]	0.227	0.189	0.371[i]
			0.033[j]
O···O–C τ[k] (deg)	33.9(7)	32.1(7)	39.3[l]
Cu–O–O–Cu (average) γ[m] (deg)	12.1	12.2	10.0
J_{exp} (cm^{-1})	+1.8	+2.9	−297.6[n]
J'_{exp} (cm^{-1})	−29.2	−32.2	

[a]The distance between adjacent copper atoms. [b]The distance between opposite copper atoms. [c]The average Cu···Cu distance within the cubane Cu_4O_4 core. [d]The average Cu···Cu distance between the capping copper and the cubane copper atoms. [e]The average θ angle of top and bottom faces of the cubane Cu_4O_4 core. [f]The average θ angle of side faces of the cubane Cu_4O_4 core. [g]The average θ angle between the capping copper and the cubane copper atoms. [h]The distortion of the coordination geometry for five-coordinated complexes is $\delta = (\alpha - \beta)/60$ (α and β are the larger *trans* X–Cu–X angles, δ is 1 for a trigonal-bipyramidal geometry and 0 for a square-pyramid).[35] [i]The average δ value of the cubane copper atoms. [j]The average δ value of the capping copper atoms. [k]τ is the substituents angle from the bridging O···O line. [l]The average τ value of the cubane copper atoms. [m]γ is the dihedral angle of the bridging O–Cu–O planes. [n]Average interactions involving the capping copper atoms and the copper atoms of the top and bottom faces of the cubane.

constant, *J*. (iii) The Cu–O–Cu angles involving the copper atoms on the top and bottom faces of the cubane, Cu1 and Cu3 and Cu2 and Cu4, respectively, present average values of 94.6° and 95.9°; therefore, a ferromagnetic interaction is expected between the copper(II) atoms. In both cases, one of the Cu–O–Cu pathways involves two apical positions on the distorted square-planar coordination sphere of the copper atoms, where the density of the unpaired electron is very small (the unpaired electron is located in the $d_{x^2-y^2}$ orbital, which lies in the basal plane and is directed to the ligand atoms coordinated to the copper atoms), and therefore they will not be operative in transmitting the exchange interaction (dotted lines in Scheme 3). For each pair of copper atoms (Cu1 and Cu3 and Cu2 and Cu4), only one magnetic pathway is operative, thus reducing the magnitude of the magnetic exchange interaction. We assume that these moderate ferromagnetic pathways are equivalent and are described by J_1. (iv) The faces involving the copper atoms Cu1 and Cu4, as well as Cu2 and Cu3, have average θ angles of 98.7° and 99.9° and one Cu-apical interaction in each magnetic pathway; therefore, weak antiferromagnetic couplings would be expected. However, the large τ angles, ∼40° and ∼50°, respectively, would lead to a weak ferromagnetic interaction. (v) The magnetic pathways involving Cu1 and Cu2 and Cu3 and Cu4 have average values of 97.6° and 96.4° and therefore weak ferromagnetic interactions are expected for them (in the latter case, there are two Cu–apical interactions reducing the magnitude of the interaction). The exchange couplings through these two magnetic pathways are considered equal and are described by J_3.

To check whether these qualitative conclusions are valid, we have simulated the magnetic properties of a system with a Cu_6O_8 core similar to that of **8** for different values of the J_1, J_2, and J_3 magnetic exchange coupling and for a fixed *J* value of -310 cm^{-1} (Figure 11) by using the following Hamiltonian:

$$\mathbf{H} = -J(S_{Cu1}S_{Cu5} + S_{Cu2}S_{Cu6} + S_{Cu4}S_{Cu6} + S_{Cu3}S_{Cu5}) - J_1(S_{Cu1}S_{Cu3} + S_{Cu2}S_{Cu4}) + J_2(S_{Cu1}S_{Cu4} + S_{Cu2}S_{Cu3}) + J_3(S_{Cu1}S_{Cu2} + S_{Cu3}S_{Cu4})$$

The following conclusions can be drawn from the simulations: (i) The high temperature data can be well reproduced with $J = -310$ cm^{-1}. The rest of the parameters do not significantly affect the shape of the curve in this temperature region. (ii) The plateau below 75 K and the further increase at a very low temperature are only observed when J_2 and J_3 are small and positive (typically both <1 cm^{-1}). If both are positive and large or one is negative and small and the other one positive and large, a wide minimum is observed below 75 K. (iii) The value of J_1 does not significantly influence the shape of the curve with either negative or positive values. (iv) If J_2 and J_3 are both negative or being both of the same magnitude either J_2 or J_3 are negative, a decrease at a very low temperature (below 10 K) is observed. The same curves are obtained for pairs of opposite values of J_2 and J_3. The data can be well reproduced with $J = -310$ cm^{-1}, $J_2 = J_3 = 0.4$ cm^{-1}, and J_1 values between -10 and 40 cm^{-1} with $g = 2.07$ (almost the same *R* values of 1.5×10^{-4} are obtained in all simulations).

Because the antiferromagnetic exchange interactions between the capping atoms Cu5 and Cu6 and the copper atoms on the top and bottom faces of the central cubane unit, Cu1 and Cu3 and Cu2 and Cu4, are very large, the spins of each pair of these latter atoms should be parallel (ferromagnetic interaction), giving rise to an $S = 1/2$ ground state for the capping isosceles triangles. Therefore from the magnetic viewpoint, the Cu_6O_8 core can be treated in a simpler manner as two isosceles triangles that interact ferromagnetically to account for the increase in $\chi_M T$ below 10 K. Taking this into account, we have fitted the magnetic data to the following simplified Hamiltonian:

dx.doi.org/10.1021/ic401325b | Inorg. Chem. 2013, 52, 11096–11109

$$\mathbf{H} = -J_A(S_{Cu1}S_{Cu5} + S_{Cu3}S_{Cu5}) - J_{1A}(S_{Cu1}S_{Cu3}) - J_B(S_{Cu2}S_{Cu6} + S_{Cu4}S_{Cu6}) - J_{1B}(S_{Cu2}S_{Cu4}) - zJ'\langle S_z\rangle S_z$$

where J_A and J_B take into account the large antiferromagnetic interactions between the capping atoms and the copper atoms at the top and bottom faces of the cubane (the two large antiferromagnetic interactions inside the isosceles triangle have been considered equal to avoid overparametrization), J_{1A} and J_{1B} describe the interactions between the latter copper atoms, and the last term accounts for the interactions between the isosceles triangles by using the molecular-field approximation. The magnetic data were fitted to the theoretical equation derived from the above Hamiltonian. Fits of a similar quality affording very close J_A and J_B values were obtained for J_{1A} and J_{1B} between zero and +40 cm^{-1}. The J_{1A} and J_{1B} do not significantly affect the fitting because their effect is only to move the energy of the excited doublet state inside the isosceles triangles. The best fit was obtained for $J_A = -335(7)$ and $J_B = -266(5)$ cm^{-1}, $g = 2.070(1)$ and $zJ' = 0.04(1)$ cm^{-1} with $J_{1A} = J_{1B} = 0$ (see Figure 11). When J_A and J_B are considered equal, the best fitting with $J_A = J_B = J$ leads to $J = -297.6(9)$ cm^{-1}, $g = 2.072(1)$, and $zJ' = 0.07$ cm^{-1}.

In order to support the sign and magnitude of the magnetic exchange interaction inside the Cu_6O_8 unit, we have carried out DFT calculations with the results given in Figure S5, Supporting Information.

The values for the interactions between the capping atoms and the copper atoms on the top and bottom faces of the cubane unit, as well as the interactions involving the atoms in these faces, agree well with those extracted from the simulation. However, the remaining interactions inside the cubane are negative and are not acceptable in view of the simulation study. At this moment, we cannot explain this unexpected result; we are undertaking new calculations using other programs and basis sets to try to resolve this discrepancy.

CONCLUSIONS

We have been able to obtain new examples of μ_4-hydroxo- and alkoxo-bridged tetranuclear copper(II) complexes $[Cu_4(\mu_4\text{-}OH)(dmae)_4][M(NO_3)_4]$ (M^I = Ag (**1**), Na (**2**), and K (**3**); dmae = *N*,*N*-dimethylaminoethanol) and the hexanuclear alkoxo-bridged "bicapped cubane" copper(II) complex $[Cu_6(ae)_8(ClO_4)_2](ClO_4)_2\cdot MeOH$ (**8**) (ae = 2-aminoethanol) via self-assembly of the corresponding aminoethanol ligand and copper(II) salt. Complexes **1**−**3** represent rare tetranuclear copper complexes with a μ_4-hydroxo bridged core, the first examples with a small amino alcohol as a ligand, whereas complex **8** is only the third example of a hexanuclear copper(II) complex with a "bicapped cubane" core. Furthermore, synthetic studies using other amino alcohol ligands revealed that a wide structural diversity of copper(II) complexes (from mononuclear to nonanuclear ones) can be obtained by varying the stoichiometry of copper(II) ion, amino alcohol, and other metal ions, as well as the nature of anions and solvents in the synthetic reaction.

Experimental magnetic studies showed that complexes **1** and **2** exhibit dominant antiferromagnetic coupling. The values of the magnetic exchange coupling constant were as follows: J = +1.8 (**1**) and +2.9 cm^{-1} (**2**) between adjacent copper atoms; J' = −29.2 (**1**) and −32.2 cm^{-1} (**2**) between opposite copper atoms.

Complex **8** exhibits a large dominant antiferromagnetic interaction between the capping copper atoms and the copper atoms of the top and bottom faces of the cubane unit that define two isosceles triangles. This interaction leads to an S =1/2 ground state for each triangle. The ferromagnetic interaction between these doublet states through the cubane unit leads to a triplet S = 1 ground state for **8**. Interestingly, in the other two examples reported in the literature as having a Cu_6O_8 core, the magnetic interactions between the copper(II) atoms lead to an S = 0 ground state. The quantitative analysis of the data with a simple model of two interacting isosceles triangles led to J = −297.6 cm^{-1} (interaction between the capping copper atoms and the copper atoms of the top and bottom faces of the cubane) and a ferromagnetic interaction between the triangles through the molecular field approximation with $zJ' = 0.07$ cm^{-1}. The magnetic coupling constants calculated for **2** and **8** by DFT methods are in general of the same nature and magnitude as the experimental ones.

ASSOCIATED CONTENT

Supporting Information

X-ray crystallographic data for all complexes in CIF format (CCDC 940671−940678), summary of the crystallographic data and selected geometrical parameters for **4**−**7**, main hydrogen bond parameters for **1**−**3** and **8**, the figure for the structure of **4**, partial crystal packing diagrams of **2** and **8**, and DFT calculated J values for **2** and **8**. This material is available free of charge via the Internet at http://pubs.acs.org.

AUTHOR INFORMATION

Corresponding Authors

*E-mail: resillan@jyu.fi. Fax: +358 14 260 1021.

*E-mail: ecolacio@ugr.es.

Notes

The authors declare no competing financial interest.

ACKNOWLEDGMENTS

We are grateful to Elina Hautakangas for performing the elemental analyses. This work was supported by MINECO, Spain (Project CTQ-2011-24478/BQU), the Junta de Andalucía, and the University of Granada. We would like to thank the Centro de Supercomputación de la Universidad de Granada for computational resources.

REFERENCES

(1) (a) Newkome, G. R.; He, E.; Moorefield, C. N. *Chem. Rev.* **1999**, *99*, 1689. (b) Leininger, S.; Olenyuk, B.; Stang, P. J. *Chem. Rev.* **2000**, *100*, 853. (c) Lu, J. Y. *Coord. Chem. Rev.* **2003**, *246*, 327. (d) Robin, A. Y.; Fromm, K. M. *Coord. Chem. Rev.* **2006**, *250*, 2127.

(2) (a) Kahn, O. *Molecular Magnetism*; VCH Publishers: New York, 1993. (b) Kahn, O. *Acc. Chem. Res.* **2000**, *33*, 647. (c) Coronado, E.; Day, P. *Chem. Rev.* **2004**, *104*, 5419.

(3) (a) Huber, R. *Angew. Chem., Int. Ed.* **1989**, *28*, 848. (b) Solomon, E. I.; Sundaram, U. M.; Machonkin, T. E. *Chem. Rev.* **1996**, *96*, 2563. (c) Gamez, P.; Aubel, P. G.; Driessen, W. L.; Reedijk, J. *Chem. Soc. Rev.* **2001**, *30*, 376. (d) Solomon, E. I.; Szilagyi, R. K.; DeBeer George, S.; Basumallick, L. *Chem. Rev.* **2004**, *104*, 419. (e) Henkel, G.; Krebs, B. *Chem. Rev.* **2004**, *104*, 801.

(4) (a) Wegner, R.; Gottschaldt, M.; Görls, H.; Jäger, E.; Klemm, D. *Chem.—Eur. J.* **2001**, *7*, 2143. (b) Díaz-Requejo, M. M.; Pérez, P. J. *Chem. Rev.* **2008**, *108*, 3379. (c) Kirillov, A. M.; Kirillova, M. V.; Pombeiro, A. J. L. *Coord. Chem. Rev.* **2012**, *256*, 2741.

(5) See, for example: (a) Bertrand, J. A.; Fujita, E.; VanDerveer, D. G. *Inorg. Chem.* **1980**, *19*, 2022. (b) Nieuwpoort, G.; Verschoor, G. C.; Reedijk, J. *J. Chem. Soc., Dalton Trans.* **1983**, 531. (c) Masi, D.; Mealli, C.; Sabat, M.; Sabatini, A.; Vacca, A.; Zanobini, F. *HeIv. Chim. Acta.* **1984**, *67*, 1818. (d) Tudor, V.; Marin, G.; Kavtsov, V.; Simonov, Y. A.; Julve, M.; Lloret, F.; Andruh, M. *Rev. Roum. Chim.* **2006**, *51*, 367.

(6) See, for example: (a) Mikuriya, M.; Nishida, Y.; Kida, S.; Uechi, T.; Ueda, I. *Acta Crystallogr., Sect. B: Struct. Crystallogr. Cryst. Chem.* **1977**, *33*, 538. (b) Merz, L.; Haase, W. *Acta Crystallogr., Sect. B: Struct. Crystallogr. Cryst. Chem.* **1978**, *34*, 2128. (c) Banci, L.; Bencini, A.; Dapporto, P.; Dei, A.; Gatteschi, D. *Inorg. Chem.* **1980**, *19*, 3395. (d) Smolander, K. *Acta Chem. Scand.* **1982**, *A36*, 589. (e) Smolander, K. *Inorg. Chim. Acta* **1987**, *128*, 61. (f) Sillanpää, R.; Lindgren, T.; Rissanen, K. *Inorg. Chim. Acta* **1987**, *134*, 233. (g) Zheng, J. C.; Rousseau, R. J.; Wang, S. *Inorg. Chem.* **1992**, *31*, 106. (h) Pinkas, J.; Huffman, J. C.; Bollinger, J. C.; Streib, W. E.; Baxter, D. V.; Chisholm, M. H.; Caulton, K. G. *Inorg. Chem.* **1997**, *36*, 2930. (i) Tudor, V.; Kravtsov, V.; Julve, M.; Lloret, F.; Simonov, Y. A.; Lipkowski, J.; Buculei, V.; Andruh, M. *Polyhedron* **2001**, *20*, 3033. (j) Vinogradova, E. A.; Vassilyeva, O. Y.; Kokozay, V. N.; Skelton, B. W. *Z. Naturforsch., B: Chem. Sci.* **2002**, *57*, 319. (k) Tudor, V.; Marin, G.; Kravtsov, V.; Simonov, Y. A.; Lipkowski, J.; Brezeanu, M.; Andruh, M. *Inorg. Chim. Acta* **2003**, *353*, 35. (l) Jocher, C.; Pape, T.; Seidel, W. W.; Gamez, P.; Reedijk, J.; Hahn, F. E. *Eur. J. Inorg. Chem.* **2005**, 4914. (m) Andruh, M. *Pure Appl. Chem.* **2005**, *77*, 1685. (n) Kirillov, A. M.; Kopylovich, M. N.; Kirillova, M. V.; Karabach, E. Y.; Haukka, M.; Guedes da Silva, M. F. C.; Pombeiro, A. J. L. *Adv. Synth. Catal.* **2006**, *348*, 159. (o) Marin, G.; Andruh, M.; Madalan, A. M.; Blake, A. J.; Wilson, C.; Champness, N. R.; Schröder, M. *Cryst. Growth Des.* **2008**, *8*, 964. (p) Gruenwald, K. R.; Kirillov, A. M.; Haukka, M.; Sanchiz, J.; Pombeiro, A. J. L. *Dalton Trans.* **2009**, 2109. (q) Kirillov, A. M.; Kirillova, M. V.; Shul'pina, L. S.; Figiel, P. J.; Gruenwald, K. R.; Guedes da Silva, M. F. C.; Haukka, M.; Pombeiro, A. J. L.; Shul'pin, G. B. *J. Mol. Catal. A: Chem.* **2011**, *350*, 26.

(7) See, for example: (a) Ferguson, G.; Langrick, C. R.; Parker, D.; Matthes, K. E. *J. Chem. Soc., Chem. Commun.* **1985**, 1609. (b) Curtis, N.; Gainsford, G.; Morgan, K. *Aust. J. Chem.* **1988**, *41*, 1545. (c) Sillanpää, R.; Rissanen, K. *Acta Chem. Scand.* **1990**, *44*, 1013. (d) Sillanpää, R.; Valkonen, J. *Acta Chem. Scand.* **1992**, *46*, 1072. (e) Myllyviita, S.; Sillanpää, R. *J. Chem. Soc., Dalton Trans.* **1994**, 2125. (f) Elerman, Y.; Kavlakoglu, E.; Elmali, A.; Kendi, E. *Z. Naturforsch., B: Chem. Sci.* **2001**, *56*, 1123. (g) Vinogradova, E. A.; Vassilyeva, O. Y.; Kokozay, V. N.; Skelton, B. W.; Bjernemose, J. K.; Raithby, P. R. *J. Chem. Soc., Dalton Trans.* **2002**, 4248. (h) Tudor, V.; Kravtsov, V. C.; Julve, M.; Lloret, F.; Simonov, Y. A.; Averkiev, B. B.; Andruh, M. *Inorg. Chim. Acta* **2005**, *358*, 2066. (i) El Fallah, M. S.; Badyine, F.; Vicente, R.; Escuer, A.; Solans, X.; Font-Bardia, M. *Chem. Commun.* **2006**, 3113. (j) Curtis, N. F.; Morgan, K. R.; Rickard, C. E. F.; Waters, J. M. *Polyhedron* **2010**, *29*, 1279. (k) Kirillov, A. M.; Karabach, Y. Y.; Kirillova, M. V.; Haukka, M.; Pombeiro, A. J. L. *Dalton Trans.* **2011**, *40*, 6378. (l) Sultan, M.; Tahir, A. A.; Mazhar, M.; Wijayantha, K. G. U.; Zeller, M. *Dalton Trans.* **2011**, *40*, 7889. (m) Maclaren, J. K.; Sanchiz, J.; Gili, P.; Janiak, C. *New J. Chem.* **2012**, *36*, 1596.

(8) See, for example: (a) Merz, L.; Haase, W. *J. Chem. Soc., Dalton Trans.* **1978**, 1594. (b) Turpeinen, U.; Ahlgrén, M.; Hämäläinen, R. *Acta Chem. Scand.* **1979**, *A33*, 593. (c) Mergehenn, R.; Merz, L.; Haase, W. *J. Chem. Soc., Dalton Trans.* **1980**, 1703. (d) Smolander, K. *Acta Chem. Scand.* **1982**, *A36*, 189. (e) Schwabe, L.; Haase, W. *J. Chem. Soc., Dalton Trans.* **1985**, 1909. (f) Turpeinen, U.; Orama, O.; Mutikainen, I.; Hämäläinen, R. *Z. Kristallogr.* **1996**, *211*, 867. (g) Whitmire, K. H.; Hutchison, J. C.; Gardberg, A.; Edwards, C. *Inorg. Chim. Acta* **1999**, *294*, 153. (h) X. Shi Tan, X.; Fujii, Y.; Nukada, R.; Mikuriya, M.; Nakano, Y. *J. Chem. Soc., Dalton Trans.* **1999**, 2415. (i) Turpeinen, U.; Klinga, M.; Mutikainen, I.; Hämäläinen, R. *Z. Kristallogr. - New Cryst. Struct.* **2000**, *215*, 418. (j) Saalfrank, R. W.; Bernt, I.; Hampel, F. *Angew. Chem., Int. Ed.* **2001**, *40*, 1700. (k) Vinogradova, E. A.; Kokozay, V. N.; Vassilyeva, O. Y.; Skelton, B. W. *Inorg. Chem. Commun.* **2003**, *6*, 82. (l) Kirillov, A. M.; Kopylovich, M. N.; Kirillova, M. V.; Haukka, M.; Guedes da Silva, M. F. C.; Pombeiro, A. J. L. *Angew. Chem., Int. Ed.* **2005**, *44*, 4345. (m) Hamid, M.; Tahir, A. A.; Mazhar, M.; Zeller, M.; Molloy, K. C.; Hunter, A. D. *Inorg. Chem.* **2006**, *45*, 10457. (n) Wang, Z.; Li, X.; Liu, B.; Tokoro, H.; Zhang, P.; Song, Y.; Ohkoshi, S.; Hashimoto, K.; You, X. *Dalton Trans.* **2008**, 2103. (o) Shahid, M.; Mazhar, M.; Hamid, M.; Zeller, M.; O'Brien, P.; Malik, M. A.; Raftery, J.; Hunter, A. D. *New J. Chem.* **2009**, *33*, 2241. (p) Shahid, M.; Mazhar, M.; Hamid, M.; O'Brien, P.; Malik, M. A.; Helliwell, M. *Appl. Organomet. Chem.* **2010**, *24*, 714. (q) Putzien, S.; Wirth, S.; Nicolas Roedel, J.; Lorenz, I. *Polyhedron* **2011**, *30*, 1747.

(9) (a) Ahlgrén, M.; Turpeinen, U.; Smolander, K. *Acta Crystallogr., Sect. B: Struct. Crystallogr. Cryst. Chem* **1980**, *36*, 1091. (b) Smolander, K. *Acta Chem. Scand.* **1983**, *A37*, 5. (c) Muhonen, H.; Hatfield, W. E.; Helms, J. H. *Inorg. Chem.* **1986**, *25*, 800. (d) Turpeinen, U.; Hämäläinen, R.; Reedijk, J. *Inorg. Chim. Acta* **1988**, *154*, 201. (e) Wang, S.; Pang, Z.; Zheng, J. C.; Wagner, M. J. *Inorg. Chem.* **1993**, *32*, 5975.

(10) (a) Escuer, A.; El Fallah, M. S.; Vicente, R.; Sanz, N.; Font-Bardia, M.; Solans, X.; Mautner, F. A. *Dalton Trans.* **2004**, 1867. (b) El Fallah, M. S.; Escuer, A.; Vicente, R.; Badyine, F.; Solans, X.; Font-Bardia, M. *Inorg. Chem.* **2004**, *43*, 7218.

(11) (a) Turpeinen, U.; Hämäläinen, R.; Reedijk, J. *Inorg. Chim. Acta* **1987**, *134*, 87. (b) El Fallah, M. S.; Escuer, A.; Vicente, R.; Badyine, F.; Solans, X.; Font-Bardia, M. *Inorg. Chem.* **2004**, *43*, 7218.

(12) See, for example: (a) Baker, W. A., Jr.; Helm, F. T. *J. Am. Chem. Soc.* **1975**, *97*, 2295. (b) Crawford, V. H.; Richardson, H. W.; Wasson, J. R.; Hodgson, D. J.; Hatfield, W. E. *Inorg. Chem.* **1976**, *15*, 2107. (c) Merz, L.; Haase, W. *J. Chem. Soc., Dalton Trans.* **1980**, 875. (d) Walz, L.; Paulus, H.; Haase, W. *J. Chem. Soc., Dalton Trans.* **1985**, 913. (e) Walz, L.; Haase, W. *J. Chem. Soc., Dalton Trans.* **1985**, 1243. (f) Lindgren, T.; Sillanpää, R.; Rissanen, K.; Thompson, L. K.; O'Connor, C. J.; Van Albada, G. A.; Reedijk, J. *Inorg. Chim. Acta* **1990**, *171*, 95. (g) Chung, Y.; Wei, H.; Liu, Y.; Lee, G.; Wang, Y. *J. Chem. Soc., Dalton Trans.* **1997**, 2825. (h) Escovar, R. M.; Thurston, J. H.; Ould-Ely, T.; Kumar, A.; Whitmire, K. H. *Z. Anorg. Allg. Chem.* **2005**, *631*, 2867. (i) Andruh, M. *Chem. Commun.* **2007**, 2565. (j) Kirillov, A. M.; Karabach, Y. Y.; Haukka, M.; Guedes da Silva, M. F. C.; Sanchiz, J.; Kopylovich, M. N.; Pombeiro, A. J. L. *Inorg. Chem.* **2008**, *47*, 162. (k) Farrugia, L. J.; Middlemiss, D. S.; Sillanpää, R.; Seppälä, P. *J. Phys. Chem. A* **2008**, *112*, 9050. (l) Seppälä, P.; Colacio, E.; Mota, A. J.; Sillanpää, R. *Inorg. Chim. Acta* **2010**, *363*, 755. (m) Seppälä, P.; Colacio, E.; Mota, A. J.; Sillanpää. *Dalton Trans.* **2012**, *41*, 2648.

(13) See, for example: (a) Astheimer, H.; Haase, W. *J. Chem. Phys.* **1986**, *85*, 1427. (b) Handa, M.; Koga, N.; Kida, S. *Bull. Chem. Soc. Jpn.* **1988**, *61*, 3853. (c) Ruiz, E.; Alemany, P.; Alvarez, S.; Cano, J. *J. Am. Chem. Soc.* **1997**, *119*, 1297. (d) Ruiz, E.; Alemany, P.; Alvarez, S.; Cano, J. *Inorg. Chem.* **1997**, *36*, 3683. (e) Hu, H.; Zhang, D.; Chen, Z.; Liu, C. *Chem. Phys. Lett.* **2000**, *329*, 255. (f) Hu, H.; Liu, Y.; Zhang, D.; Liu, C. *THEOCHEM* **2001**, *546*, 73. (g) Hu, H.; Yang, X.; Chen, Z. *THEOCHEM* **2002**, *618*, 41. (h) Rodríguez-Fortea, A.; Ruiz, E.; Alemany, P.; Alvarez, S. *Monatsh. Chem.* **2003**, *134*, 307. (i) Tercero, J.; Ruiz, E.; Alvarez, S.; Rodríguez-Fortea, A.; Alemany, P. *J. Mater. Chem.* **2006**, *16*, 2729. (j) Ruiz, E.; Rodríguez-Fortea, A.; Alemany, P.; Alvarez, S. *Polyhedron* **2001**, *20*, 1323. (k) Calzado, C. J.; Maynau, D. *J. Chem. Phys.* **2011**, *135*, No. 194704.

(14) (a) Melník, M.; Kabešová, M.; Koman, M.; Macáškova, L.; Holloway, C. E. *J. Coord. Chem.* **1999**, *48*, 271. (b) Melník, M.; Koman, M.; Ondrejovič, G. *Coord. Chem. Rev.* **2011**, *255*, 1581.

(15) (a) McKee, V.; Tandon, S. S. *J. Chem. Soc., Chem. Commun.* **1988**, 385. (b) McKee, V.; Tandon, S. S. *J. Chem. Soc., Dalton Trans.* **1991**, 221. (c) Burkhardt, A.; Spielberg, E. T.; Simon, S.; Goerls, H.; Buchholz, A.; Plass, W. *Chem.—Eur. J.* **2009**, *15*, 1261. (d) Abrahams, B. F.; Haywood, M. G.; Robson, R. *Chem. Commun.* **2004**, 938.

(16) Shit, S.; Nandy, M.; Rosair, G.; Salah El Fallah, M.; Ribas, J.; Garribba, E.; Mitra, S. *Polyhedron* **2013**, *52*, 963.

(17) Otwinowski, Z.; Minor, W. In *Methods in Enzymology, Part A* Carter, C. W., Sweet, R. M., Eds.; Academic Press: New York, 1997; Vol. *276*, pp 307−326.

(18) Sheldrick, G. M., *SADABS-2008/1*, University of Göttingen, Germany.
(19) Palatinus, L.; Chapuis, G. *J. Appl. Crystallogr.* **2007**, *40*, 786.
(20) Sheldrick, G. M. *Acta Crystallogr., Sect. A: Found. Crystallogr.* **2008**, *64*, 112.
(21) Farrugia, L. J. *J. Appl. Crystallogr.* **1999**, *32*, 837.
(22) Brandenburg, K.; Putz, H.*Diamond - Crystal and Molecular Structure Visualization*, Crystal Impact, Postfach 1251, D-53002 Bonn, Germany.
(23) Macrae, C. F.; Edgington, P. R.; McCabe, P.; Pidcock, E.; Shields, G. P.; Taylor, R.; Towler, M.; van de Streek, J. *J. Appl. Crystallogr.* **2006**, *39*, 453.
(24) Becke, A. D. *Phys. Rev. A: Gen. Phys.* **1988**, *38*, 3098.
(25) Lee, C.; Yang, W.; Parr, R. G. *Phys. Rev. B: Condens. Matter* **1988**, *37*, 785.
(26) Becke, A. D. *J. Chem. Phys.* **1993**, *98*, 5648.
(27) Frisch, M. J.; Trucks, G. W.; Schlegel, H. B.; Scuseria, G. E.; Robb, M. A.; Cheeseman, J. R.; Montgomery, J. A., Jr.; Vreven, T.; Kudin, K. N.; Burant, J. C.; Millam, J. M.; Iyengar, S. S.; Tomasi, J.; Barone, V.; Mennucci, B.; Cossi, M.; Scalmani, G.; Rega, N.; Petersson, G. A.; Nakatsuji, H.; Hada, M.; Ehara, M.; Toyota, K.; Fukuda, R.; Hasegawa, J.; Ishida, M.; Nakajima, T.; Honda, Y.; Kitao, O.; Nakai, H.; Klene, M.; Li, X.; Knox, J. E.; Hratchian, H. P.; Cross, J. B.; Bakken, V.; Adamo, C.; Jaramillo, J.; Gomperts, R.; Stratmann, R. E.; Yazyev, O.; Austin, A. J.; Cammi, R.; Pomelli, C.; Ochterski, J. W.; Ayala, P. Y.; Morokuma, K.; Voth, G. A.; Salvador, P.; Dannenberg, J. J.; Zakrzewski, V. G.; Dapprich, S.; Daniels, A. D.; Strain, M. C.; Farkas, O.; Malick, D. K.; Rabuck, A. D.; Raghavachari, K.; Foresman, J. B.; Ortiz, J. V.; Cui, Q.; Baboul, A. G.; Clifford, S.; Cioslowski, J.; Stefanov, B. B.; Liu, G.; Liashenko, A.; Piskorz, P.; Komaromi, I.; Martin, R. L.; Fox, D. J.; Keith, T.; Al-Laham, M. A.; Peng, C. Y.; Nanayakkara, A.; Challacombe, M.; Gill, P. M. W.; Johnson, B.; Chen, W.; Wong, M. W.; Gonzalez, C.; Pople, J. A. *Gaussian 03*, revision C.02; Gaussian, Inc.: Wallingford, CT, 2003.
(28) Bacskay, G. B. *Chem. Phys.* **1981**, *61*, 385.
(29) Schäfer, A.; Huber, C.; Ahlrichs, R. *J. Chem. Phys.* **1994**, *100*, 5829.
(30) *Jaguar 7.6*; Schrödinger, Inc.: Portland OR, 2009.
(31) Ruiz, E.; Cano, J.; Alvarez, S.; Alemany, P. *J. Comput. Chem.* **1999**, *20*, 1391.
(32) Ruiz, E.; Alvarez, S.; Rodríguez-Fortea, A.; Alemany, P.; Pouillon, Y.; Massobrio, C. *Magn.: Mol. Mater. II* **2001**, 227−279.
(33) Ruiz, E.; Rodríguez-Fortea, A.; Cano, J.; Alvarez, S.; Alemany, P. *J. Comput. Chem.* **2003**, *24*, 982.
(34) Ruiz, E.; Alvarez, S.; Cano, J.; Polo, V. *J. Chem. Phys.* **2005**, *123*, No. 164110.
(35) Addison, A. W.; Rao, T. N.; Reedijk, J.; van Rijn, J.; Verschoor, G. C. *J. Chem. Soc., Dalton Trans.* **1984**, 1349.
(36) Borrás-Almenar, J. J.; Clemente-Juan, J. M.; Coronado, E.; Tsukerblat, B. S. *J. Comput. Chem.* **2001**, *22*, 985.
(37) Patra, A. K.; Ray, M.; Mukherjee, R. *Polyhedron* **2000**, *19*, 1423.
(38) Arora, H.; Cano, J.; Lloret, F.; Mukherjee, R. *Dalton Trans.* **2011**, *40*, 10055.